UCSF
UC San Francisco Electronic Theses and Dissertations

Title

Investigating the effects of tau acetylation on stability of cytoskeleton in the axon initial segment

Permalink

https://escholarship.org/uc/item/8rj6h1fh

Author

Sohn, Peter Dongmin

Publication Date

2015

Peer reviewed|Thesis/dissertation

Investigating the effects of tau acetylation
on stability of cytoskeleton in the axon initial segment

by

Peter Dongmin Sohn

DISSERTATION

Submitted in partial satisfaction of the requirements for the degree of

DOCTOR OF PHILOSOPHY

in

Neuroscience

in the

GRADUATE DIVISION

of the

ACKNOWLEDGEMENTS

CONTRIBUTIONS

Chapters 2, 3, and 5 have largely appeared in my submitted manuscript in July, 2015. Tara Tracy collaborated by generating the transgenic mice. Chao Wang optimized cultures of iPSC-derived neurons. Yungui Zhou supported mouse maintenance and biochemical experiments. Hye-In Son and Justin Baik were student interns who assisted data acquisition and analyses. Lisa Ellerby and Bradford Gibson collaborated by performing mass spectrometry analyses. Lea Grinberg collaborated by performing immunohistochemistry of human brains. Li Gan was the principal investigator who supervised the project and assisted with the writing of the submitted manuscript.

ABSTRACT

Investigating the effects of tau acetylation
on stability of cytoskeleton in the axon initial segment

Peter Dongmin Sohn

Neurons are highly polarized cells in which asymmetric axonal-dendritic distribution of proteins is crucial for neuronal function. Somatodendritic mislocalization of the axonal protein tau is an early sign of Alzheimer's disease (AD) and other neurodegenerative disorders. However, the pathogenic molecular mechanisms are incompletely understood. Here we report that tau acetylation and consequent destabilization of the axon initial segment (AIS) cytoskeleton are important in the somatodendritic mislocalization of tau. AD-relevant acetylation at K274 and K281 in the microtubule (MT)-binding domain of tau reduced tau binding to MTs. In primary neuronal cultures, acetylation at these sites led to hyperdynamic MTs in the AIS, shown by live-imaging of MT mobility and fluorescence recovery after photobleaching. AIS cytoskeletal proteins, including ankyrin G and βIV-spectrin, were downregulated in AD brains and in the brains of transgenic mice expressing tauK274/281Q, which mimics acetylation. Using photoconvertible tau constructs, we found that acetylated axonal tau is mislocalized to the somatodendritic compartment. Stabilizing MTs with epothilone D to restore the cytoskeletal barrier in the AIS prevented tau mislocalization in primary neuronal cultures. These findings suggest that tau acetylation contributes to neurodegenerative disease by compromising the cytoskeletal sorting machinery in the AIS. Finally, characterization of the AIS in human iPSC-derived neurons reveals aberrant AIS location and impaired AIS plasticity in neurons with pathogenic tau mutation.

TABLE OF CONTENTS

List of Figures and Table

CHAPTER 1

Introduction / Literature Review

Pathogenic tau in neurodegenerative diseases

Tau protein is encoded by *MAPT*, a gene located on chromosome 17. Different splice variants of *MAPT* produce multiple isoforms of tau, six of which are common in the human central nervous system. These isoforms differ by the presence of exons 2 and 3 (0N, 1N, and 2N) and possess either three or four microtubule (MT)-binding repeat motifs (3R or 4R). Tau protein accumulates pathologically in several neurodegenerative disorders, collectively termed tauopathies (Lee et al., 2001). Neurofibrillary tangles (NFTs) and amyloid plaques are the hallmarks of Alzheimer's disease (AD). NFTs are composed of aggregated, hyperphosphorylated tau found in neurons (Brion, 1992). Although the amyloid cascade hypothesis predicts that amyloid-beta (Aβ) is the central upstream trigger for AD pathology (Hardy and Higgins, 1992), clinical and pathological evidence has shown that Aβ plaque burden does not correlate with cognitive decline (Dickson et al., 1991; Delaere et al., 1991; Arriagada et al., 1992; Berg et al., 1993). Instead, tau has been shown to be the critical effector of AD pathology (Lewis et al., 2001; Roberson et al., 2007; Ittner et al., 2010). Accumulation of tau is independent of Aβ deposits in other tauopathies such as frontotemporal dementia (FTD) and chronic traumatic encephalopathy (CTE) (Iqbal et al., 2005; Baugh et al., 2012). These studies suggest that tau has a significant role in cognitive dysfunction.

Although mutations in tau do not cause AD, many mutations found in other tauopathies have enhanced our understanding of tau biology. These mutations have largely discovered through family genetic studies of patients who have FTD with parkinsonism linked to chromosome 17 (FTDP-17). The mutations segregate into two groups, which have different

biological consequences. The first group consists of intronic mutations, which affect the splicing of exon 10 (Hutton et al., 1998). Exon 10 encodes one of the MT-binding repeats whose presence or absence leads to 3R or 4R tau. The normal ratio of 3R to 4R tau in the adult brain is 1:1; therefore, mutations that modify this ratio alter MT stability and tau aggregation. The second group of mutations is found in the coding region of the MT-binding domain and hence alters tau's affinity for MTs. Other tau mutations cause progressive supranuclear palsy (PSP) and corticobasal degeneration (CBD), both of which are largely sporadic (Dickson et al., 2007). The changes in tau pathology are similar in these diseases, resulting in both a loss-of-function of tau by reducing MT stability and a gain-of-function of tau by enhancing its aggregation into filamentous inclusions.

Tau loss-of-function vs gain-of-function

Loss of tau function leads to destabilization of MTs and deficits in axonal transport and has been implicated in AD pathogenesis (Lee and Cleveland, 1994). MT-stabilizing drugs, such as paclitaxel and epothilone D, reverse axonal transport deficits and cognitive impairment in transgenic mice of tauopathy (Zhang et al., 2005; Zhang et al., 2012). Interestingly, tau knockout mice are phenotypically normal, suggesting that loss of tau function may not be a primary driver of cognitive decline. Notably, genetic reduction of endogenous tau prevents Aβ toxicity *in vivo*, suggesting that tau is necessary for Aβ-induced cognitive deficits and is therefore a key facilitator of neurodegeneration (Roberson et al., 2007; Ittner et al., 2010). Crossing a model of mutant human APP with a mouse tau knockout line rescues memory deficits, increased mortality, and excitotoxic seizures (Roberson et al., 2007). Similarly, crossing a tau knockout mouse with the APP233 mouse produces a comparable rescue of memory and mortality. The tau knockout mice prevents postsynaptic targeting of the protein kinase Fyn, which underlies synaptic tethering of PSD-95 and NMDA receptors (Ittner et al.,

2010). These studies indicate that tau gain-of-function is responsible for excitotoxicity and cognitive decline.

Post-translational modifications of tau

Tau phosphorylation

Hyperphosphorylated tau that is oligomeric and nonfilamentous precedes and promotes the formation of paired helical filaments (PHFs) (Bancher et al., 1989), making it an important marker of disease progression. In patients with mild cognitive impairment, the levels of phosphorylated tau in cerebrospinal fluid are strongly associated with subsequent development of AD (Hansson et al., 2006; Mattsson et al., 2009). In mouse models of tauopathies, tau hyperphosphorylation correlates with cognitive decline and tangle formation. In transgenic mice with glycogen synthase kinase-3β (GSK-3β) overexpression, increased tau phosphorylation is associated with neurodegeneration and spatial learning deficits, which are independent of filament formation (Hernandez et al., 2002). In double transgenic mice with overexpression of the cyclin-dependent kinase 5 (cdk5) activator p25 and human tau with mutant (P301L) human tau, enhanced cdk5 activity is associated with hyperphosphorylation of tau and accumulation of aggregated tau accompanied by increased numbers of NFTs (Noble et al., 2003).

Tau has 85 sites that can be phosphorylated, including 80 serines/threonines and 5 tyrosines. More than 40 phosphorylation sites have been detected in AD brains by mass spectrometry and antibodies targeting specific phosphorylated tau species (Stoothoff and Johnson, 2005). GSK-3β, cdk5, casein kinase 1 (CK1), and cAMP-dependent protein kinase A (PKA) are the kinases that are most extensively studied and are considered the most promising for regulating tau hyperphosphorylation (Ishiguro et al., 1993; Ishiguro et al., 1994; Jicha et al., 1999). GSK-3β and cdk5 can phosphorylate at most of known sites found in AD

(Gong et al., 2005). PP2A is a major phosphatase accounting for more than 70% of de-phosphorylated tau at most of its phosphorylation sites (Liu et al., 2005). In AD brains, PP2A activity is significantly reduced and de-phosphorylation of tau PP2A inhibits PHF formation and restores MT stability (Gong et al., 1995). These beneficial changes can be reversed by phosphorylation by GSK-3β, cdk5, and PKA (Wang et al., 2007).

Consequences of hyperphosphorylation of tau include its detachment from MTs, dendritic mislocalization, and aggregation. Phosphorylation at S262/356 in the KXGS motifs of the MT-binding domain reduces tau binding for MTs and results in diffusion of MT-unbound tau to the somatodendritic compartment (Li et al., 2011). The pseudophosphorylated tau in which 14 disease-related serines and threonines are mutated to mimic phosphorylation is mislocalized to dendritic spines and causes a decrease in spontaneous synaptic transmission (Hoover et al., 2010). Hyperphosphorylation inhibits the proteasomal degradation (Ren et al., 2007). Notably, phosphorylation at the KXGS motif renders tau unrecognizable by the proteasome machinery, including CHIP and Hsp70/90 chaperone complex, making tau species prone to accumulate (Dickey et al., 2007).

Tau acetylation

Tau undergoes lysine acetylation, which modulates diverse biological processes including protein stability and protein-protein interactions (Kim and Yang, 2011). Analyses of soluble fraction of AD brain lysates show that tau acetylation is enhanced in patients at early/moderate Braak stages, an early role of acetylation in modulating tau accumulation (Min et al., 2010). Tau acetylation at lysines competes with polyubiquitination and slows down its turnover in primary neurons. Acetylation state can be regulated by the histone acetyltransferase p300 and the deacetylase sirtuin 1 (SIRT1) (Min et al., 2010). Systems biology approach to figure out dysregulated genetic networks in AD reveals increase in p300 acetyltransferase activity in AD cases (Aubry et al., 2015). Accumulating evidence has

confirmed tau acetylation and uncovered specific lysine residues whose acetylation leads to site-specific consequences on tau biology (Min et al., 2010; Cohen et al., 2011; Irwin et al., 2012; Grinberg et al., 2013; Cook et al., 2014; Min et al., 2015). Mass spectrometry reveals K174 acetylation in soluble fraction of AD brains. K174 acetylation leads to accumulation of tau monomers that are associated with cognitive deficits. Inhibition of p300 acetyltransferase lowers acetylated K174 tau and protects against cognitive deficits, hippocampal atrophy, and accumulation of NFTs in a mouse model of FTD with expression of human P301S tau (Min et al., 2015).

Acetylation of the 6 amino acid motif VQIINK (K280) that is critical for the formation of tau oligomers and filaments reduces tau binding to MTs and promotes tau aggregation (Cohen et al., 2011). Acetylated K280 is found in patient brains of AD and other tauopathies such as corticobasal degeneration (CBD) and progressive supranuclear palsy (PSP). In AD brains, acetylated K280 is located in intracellular thioflavin-S-positive tau inclusions while it is also found in thioflavin-S-negative pathology in CBD and PSP. The distribution pattern of acetylated K280 is similar to that of hyperphosphorylated tau (Irwin et al., 2012). Interestingly, intrinsic acetyltransferase activity of tau can lead to self-acetylation of K280 acetylation (Cohen et al., 2013).

Acetylation of KXGS motifs in the MT-binding domain inhibits phosphorylation on the same motif (S262/356) and prevents tau aggregation. In AD brains and a mouse model of tauopathy (rTg4510), KXGS motifs are hypoacetylated and hyperphosphorylated. The histone deacetylase 6 (HDAC6) appears to regulate acetylation state of KXGS motifs (Cook et al., 2014).

Acetylation of K274 is found in tau inclusions of various tauopathies including AD, CBD, PSP, Pick's disease, and chronic traumatic encephalopathy. Interestingly, argyrophilic grain disease (AGD), which is common but atypical tauopathy not always associated with clinical

progression, lacks tau acetylation at K274. This finding raises the hypothesis that tau acetylation at K274 could be a key modification for the propagation of tau toxicity (Grinberg et al., 2013). Tau acetylation of K281 is also found in AD brains and a mouse model of FTD. Moreover, a recent study detects acetylation of K281 tau in human APP transgenic mice (Morris et al., 2015). Acetylated K274/281 tau disrupts postsynaptic actin dynamics and AMPAR insertion required for LTP expression. Transgenic mice expressing human tau with lysine-to-glutamine mutations to mimic K274/281 acetylation exhibit AD-related memory deficits and impaired hippocampal LTP. These findings implicate that acetylated K274/281 tau is involved in a postsynaptic mechanism by which tau inhibits synaptic plasticity and promotes cognitive decline in AD pathogenesis (Tracy et al., unpublished observations).

Overall, the acetylation profile of tau is regulated by multiple enzymes, and the functional consequences of tau acetylation appear to be site-specific. The importance of tau acetylation in regulating its degradation, aggregation, phosphorylation, and synaptic plasticity in the pathogenic conditions suggests novel therapeutic opportunities for targeting pathogenic tau species.

Tau missorting

Neurons are highly polarized cells in which asymmetric axonal-dendritic distribution of cellular contents are crucial for proper neuronal functions. Unlike other microtubule-associated proteins (MAPs), tau is preferentially distributed in axons under physiological conditions in adult brains. During embryonic development, the fetal 3R-tau isoform (0N3R) is initially distributed all over the subcellular compartments. As neurons establish their polarity, tau becomes enriched in axons (Mandell and Banker, 1995; Bullmann et al., 2009).

Tau sorting mechanisms

How is tau preferentially distributed in axons? Several mRNA-based and protein-based

mechanisms may work in parallel to maintain tau distribution in axons. On the mRNA level, selective transport and translation of tau mRNA in axons have been proposed to demonstrate axonal distribution of tau. The 3'-untraslated region (3'-UTR) axonal localization signal of tau mRNA governs selective transport of tau mRNA into axons (Aronov et al., 2001). Local translation of tau mRNA in axons occurs owing to the 5'-UTR oligopyrimidine tract sequences that mediate mTOR-mediated protein synthesis in axons (Morita and Sobue, 2009). On the other hand, protein-based mechanisms for axonal retention of tau include preferential tau binding to axonal MTs and the diffusion barrier that maintains tau in axons. MT binding affinity of tau is higher in axons than in dendrites, leading to trapping of tau bound to axonal MTs (Kanai and Hirokawa, 1995; Hirokawa et al., 1996). This difference of tau binding to axonal and dendritic MTs can be explained by differential post-translational modifications of tau and MTs in axons and dendrites. For instance, axonal tau is less phosphorylated at the KXGS motifs. When phosphorylated at these sites, polarized distribution of tau in axons is lost because phosphorylated tau detaches from the axonal MTs and becomes readily diffusible to the dendritic compartment (Schneider et al., 1999). Given that tau has a net positive charge, higher levels of negatively charged polyglutamylation of tubulin in axons than in dendrites may also keep tau bound to axonal MTs (Janke and Kneussel, 2010). Axonal retention of tau can be explained by a tau diffusion barrier in the axon initial segment (AIS) that is located between the soma and axon (Li et al., 2011). Cytoskeletal network in the AIS has been described as selective filter that controls protein transport (Rasband, 2011). Notably, MTs in the AIS prevent retrograde invasion of axonal tau to the somatodendritic compartment (Li et al., 2011).

Tau missorting in patholgocal conditions

In AD brains, NFTs which are composed of tau aggregates and hyperphosphorylated tau are found mainly in the somatodendritic compartment of neurons, where abnormally

phosphorylated tau is mislocalized at an early stage of pathology. Thus, it is speculated that missorting of tau is important in tau pathology and contributes to cognitive deficits. Indeed, the formation of NFTs in the somatodendritic compartment and the phosphorylation of missorted tau have been used as diagnostic criteria and staging of disease progression in AD (Braak and Braak, 1991; Braak et al., 2006). In FTDP-17, mutations in the tau gene cause tau pathology including missorting of tau, which is associated with motor deficits and cognitive decline (Goedert et al., 2012). In other tauopathies including Pick disease (PiD), corticobasal degeneration (CBD), and progressive supranuclear palsy (PSP), tau is mislocalized in other cellular compartments than the axons (Dickson et al., 2011). Therefore, tau mislocalization outside the axons is common phenotype observed in various neuropathological conditions.

Several mouse models that express human tau have been generated to study the missorting of tau in relation to its phosphorylation, aggregation, and pathology. In a model with slight (<10%) overexpression of the longest isoform of human tau, tau is hyperphosphorylated and missorted into the somatodendritic compartment (Gotz et al., 1995). Twofold overexpression of mouse tau also leads to tau missorting and phosphorylation of tau (Adams et al., 2009). In contrast, in a tau knockout-knockin model in which human tau with levels comparable to that of endogenous mouse tau is expressed in the mouse tau knockout background, tau is not missorted and no obvious pathology is observed even when the FTDP-17 mutation P301L is introduced (Terwel et al., 2005). Tau overexpression in primary neuronal culture induces missorting of exogenous tau as well as endogenous murine tau (Li et al., 2011). Thus, tau missorting in animal models and cell culture can simply be achieved by overexpression of tau. It is conceivable that tau may be missorted under pathological conditions when homeostasis regulating tau levels is perturbed.

What triggers tau missorting to the somatodendritic compartment in diseased brains? Depositions of Aβ and tau protein are hallmarks of AD. Aβ is considered toxic for neurons

and tau a downstream mediator of the Aβ cascade. In primary neuronal cultures, exposure to Aβ readily induces tau mislocalization to the somatodendritic compartment (Busciglio et al., 1995; Zempel et al., 2010; Zempel et al., 2013). A mechanism underlying Aβ-induced tau missorting involves elevation of intracellular Ca^{2+}. Ca^{2+} influx-inducing stressors such as glutamate and ATP are also sufficient to mislocalize tau to the somatodendritic compartment, suggesting the importance of impairment of Ca^{2+} signaling in tau missorting (Zempel et al., 2010; Zempel et al., 2013).

Consequences of tau missorting

Loss of dendritic MTs and spines. Mice overexpressing wildtype or mutant tau show dendritic missorting of tau and destabilization of MTs (Zhang et al., 2012). In cultured neurons overexpressing tau, missorting of tau accompanies with loss of dendritic microtubules and disappearance of spines (Thies and Mandelkow, 2007). Loss of dendritic MTs depends on the presence of tau, or correlates with dendritic missorting of tau (King et al., 2006; Zempel et al., 2010). These observations appear to be contradictory to the MT-stabilizing function of tau. Although MT stabilization is one of suggested functions of tau, tau knockout mice show no MT-related deficits except for only mild changes in neurite extension (Dawson et al., 2001). In fact, tau knockout mice even show protective effects against Aβ-induced cognitive impairment, excitotoxicity, and deficits in axonal transport (Roberson et al., 2007; Ittner et al., 2010; Vossel et al., 2010). These findings suggest that loss of function of tau is not sufficient to explain the breakdown of MTs. Instead, tau may have an active role in loss of dendritic MTs. Missorted tau disrupts dendritic MTs by recruiting the MT-severing enzyme spastin to the dendrites. Tau-dependent translocation of tubulin tyrosine ligase-like enzyme 6 (TTLL6) and subsequent polyglutamylation of dendritic MTs trigger the recruitment of the spastin which severs MTs in dendrites (Lacroix et al., 2010; Zempel et al., 2013).

Altered tau phosphorylation. Axonal tau is highly phosphorylated at the PHF-1 epitope

(S396/S404), whereas missorted tau in the somatodendritic compartment is highly phosphorylated at the 12E8 epitope (S262 in the KXGS motif in the repeat domain) (Zempel et al., 2010). This difference in phosphorylation status primarily reflects an asymmetric distribution of tau phosphatases and tau kinases. PP2A, a major tau phosphatase that is predominantly responsible for the dephosphorylation of S262, is preferentially localized in axons (Zhu et al., 2010). On the other hand, kinases such as MARK and SAD, which are mainly responsible for the phosphorylation in the repeat domain, are localized in dendrites and spines (Kishi et al., 2005; Hayashi et al., 2011). The sorting of those kinases and phosphatases leads to differences in the phosphorylation status of the 12E8 epitope. Conversely, the preferential phosphorylation of the PHF-1 epitope is caused by the ubiquitous presence of GSK3β and the dendritic localization of PP2b, the kinase/phosphatase pair responsible for phosphorylation at S396/S404 (Martin et al., 2013). Alterations in tau phosphorylation can change its profiles of tau-interacting partners. Of note, it is possible that the association with synaptic membranes and postsynaptic receptors may be altered, resulting in synaptic dysfunction (Hoover et al., 2010; Pooler et al., 2012; Mondragon-Rodriguez et al., 2012).

Synaptic dysfunction. Translocation of dendritic tau into spine heads is a characteristic feature observed in pathological conditions, including AD (Tai et al., 2012). In primary neuronal cultures, strong expression of tau by adenovirus leads to translocation of tau in spines (Thies and Mandelkow, 2007). At lower expression levels, P301L tau mutation leads to tau mislocalization in dendritic spines (Hoover et al., 2010). Increased synaptic input can trigger postsynaptic mislocalization of tau (Frandemiche et al., 2014). Once localized in the postsynaptic compartment, tau is involved in postsynaptic targeting of the Src kinase Fyn, which in turn stabilizes the complex of the NMDM receptors and PSD-95 in the postsynaptic density. This coupling of the NMDA receptors and PSD-95 underlies Aβ-induced

excitotoxicity, which can be prevented by removing tau (Ittner et al., 2010). The P301L tau mutation impairs glutamate receptor trafficking and synaptic anchoring (Hoover et al., 2010). Postsynaptic tau interacts with F-actin, the most predominant cytoskeleton whose dynamics is essential for synaptic plasticity (Frandemiche et al., 2014). Acetylation of tau at K274 and K281 disrupts activity-dependent dynamics of postsynaptic F-actin, resulting in impaired AMPA receptor insertion and LTP deficits (Tracy et al., unpublished observations).

Tau-mediated alterations of neuronal cytoskeleton

Microtubule and actin cytoskeleton

MT stabilization was initially proposed as a primary function of tau in cell-free conditions (Weingarten et al., 1975). Although MT-binding activity of tau promotes MT stability and assembly *in vitro*, recent studies have challenged this notion that MT stabilization is a critical function of tau. The population of tau-bound MTs exhibits the highest basal turnover rate of any MT populations in primary cultures and mouse hippocampus *in vivo* (Fanara et al., 2010). Genetic reduction of tau does not alter cargo transport along axonal MTs (Yuan et al., 2008) but rather prevents Aβ-induced deficits in axonal transport (Vossel et al. 2010).

Excessive tau interferes with binding of motor proteins to MTs (Dixit et al., 2008) and FTDP-17 mutations of tau leads to reduction of MT density (Zhang et al., 2005; Zhange et al., 2012) and increase in MT dynamics (Barten et al., 2012). Given that neutral or protective effect of lowering tau on MT stability and functions, these findings of tau-mediated destabilization of MTs are likely to be explained by a gain-of-function of tau rather than a simple loss of MT stabilization function of tau.

This active role of tau in altering cytoskeleton has been further supported by the study on mislocalizaed dendritic tau that induces severing of dendritic MTs. Recruitment of MT-severing enzyme spastin depends on tau-mediated translocation of TTLL6 (Zempel et al.,

2013). Tau can also interact with other cytoskeleton such as actin filament in neurons. This interaction between tau and the actin filament induces abnormal F-actin bundling and accumulation in brains (Fulga et al., 2007; He et al., 2009). Furthermore, mislocalized postsynaptic tau can interact with F-actin in spines (Frandemiche et al., 2014) and inhibits activity-dependent actin dynamics, leading to deficits in LTP (Tracy et al., unpublished observations). It is possible that tau may play a role in connecting MTs and actin cytoskeletal networks (Farias et al., 2002).

AIS cytoskeleton

Characteristics of neuronal cytoskeleton vary depending on subcellular compartment. Notably, the axon initial segment (AIS) is located between the axon and the somatodendritic compartment and its unique cytoskeletal proteins are composed of MT bundles coated with a dense submembrane protein network containing ankyrin G (AnkG), βIV-spectrin, and actin filaments (Palay et al., 1968; Jones et al., 2014). MTs and AnkG are physically and functionally connected by end-binding proteins EB1 and EB3 in the AIS (Leterrier et al., 2011). The AIS plays an essential role in generation of action potentials and maintenance of neuronal polarity. Ion channels such as voltage-gated sodium and potassium channels that are responsible for firing action potentials are anchored to the scaffolding proteins, including AnkG and βIV-spectrin (Rasband, 2010). Genetic ablation of AnkG or βIV-spectrin results in failure of recruiting the AIS cytoskeleton and ion channels to the AIS (Jenkins and Bennett, 2001; Komada and Soriano, 2002; Hedstrom et al., 2008). The AIS cytoskeleton forms a barrier between the axon and the somatodendritic membrane (Winckler et al., 1999) and regulates axonal entry of cargoes that require selective transport (Song et al., 2009).

The AIS barrier, MTs in particular, contributes to the retention of tau in axons by preventing its retrograde invasion to the somatodendritic compartment. Pathologically modified tau that has weak binding affinity for MTs can bypass the AIS barrier and be

mislocalized from the axon to the dendrites (Li et al., 2011). Recent studies have provided evidence that the AIS barrier is perturbed in AD pathogenesis. Primary cultures from AD mouse models show decreased expression of AnkG, disrupting AIS localization of sodium channels and dendritic localization of NR2B. The exogenous expression of AnkG improves cognitive performance of an AD mouse model (Sun et al., 2014). When exposed to Aβ, primary neurons display inhibition of HDAC6, resulting in mislocalization of AnkG and increased MT instability in the AIS (Tsushima et al., 2015).

The AIS regulates intrinsic excitability of neurons and maintain its homeostasis in response to changes in neuronal activity. Mutations of ion channels in the AIS proteins can lead to synchronized firing of neuronal network such as epilepsy (Wimmer et al., 2010). In response to increased activity in primary culture, the location of the AIS is shifted distally in axons. The distal shift of the AIS location is associated with reduced excitability of neurons (Grubb et al., 2010). In contrast, removal of sensory input to chick auditory neurons leads to increase in the length of the AIS (Kuba et al., 2010). Activation of calcineurin mediates this activity-dependent AIS plasticity (Evans et al., 2013). Several recent independent studies have demonstrated that tau modulates neuronal excitability. Genetic ablation of tau attenuates network hyperexcitability (Roberson et al., 2011; Holth et al., 2013; DeVos et al., 2013). Given the tau's role in regulating neuronal excitability, it is possible that tau may play a role in determining the AIS location and length and cytoskeletal rearrangement in the AIS in response to changes in neuronal activity.

Summary and objectives

NFTs of hyperphosphorylated tau are major hallmarks of neurodegenerative diseases such as AD. Mutations of tau gene can cause a variety of tauopathies, including FTD, PSP, CBD, and PiD. Tau has an active detrimental role in eliciting toxicity and cognitive decline. Notably,

somatodendritic mislocalization of tau is a key early event in the pathogenesis of neurodegenerative diseases. Adverse consequences of tau missorting into the dendrites include loss of dendritic MTs and spines, altered tau phosphorylation state, and synaptic dysfunction. Lysine acetylation of tau can affect its turnover, aggregation, synaptic plasticity, and cytoskeletal stability. The AIS cytoskeleton is essential for maintaining polarized distribution of proteins in neurons. However, the functional significance of tau acetylation in regulating the AIS cytoskeleton is not well characterized.

In this study, we sought to determine which lysine residues are acetylated in human AD brains and whether AD-relevant tau acetylation affects the stability of the AIS cytoskeleton in cultured cells and *in vivo*. To measure dynamics of AIS cytoskeleton in neuronal cultures, we took advantage of using EB proteins tagged with GFP for live imaging and performed fluorescence recovery after photobleaching (FRAP) with GFP-tagged tubulin. To test the hypothesis that changes in the AIS cytoskeleton lead to somatodendritic mislocalization of tau, we used photoconvertible tau constructs and monitored movement of tau after photoconversion in neuronal cultures. We then assessed pharmacological stabilization of MTs as a strategy to preserve the axonal distribution of tau and reduce pathological features. Finally, AIS plasticity of iPSC-derived human neurons was analyzed to compare neurons derived from control groups and patients with the FTDP-17 tau mutation.

CHAPTER 2

Materials and Methods

Plasmids. cDNA encoding 2N4R human tau was cloned into pEGFP-C1 vector (Clontech). In mApple-tagged tau plasmids, EGFP in the pEGFP-C1 vector was replaced with mApple. Tau mutations (K163/174/180/190Q, K274Q, K281Q, K274/281Q, and K274/281R) were generated with the QuickChange mutagenesis kit (Stratagene). The following plasmids were gifts: GFP-tubulin (Dr. Ron Vale, University of California, San Francisco), GFP-end-binding protein (EB) 1 (Dr. Torsten Wittmann, University of California, San Francisco), and GFP-EB3 (Dr. Niels Galjart, Erasmus MC, Rotterdam).

Mice. The murine prion promoter (Mo.PrP) expression plasmid (Mo.PrP.Xho) has been previously described (Borchelt et al., 1996). Human tau cDNA (2N4R) with A820C (K274Q) and A841C (K281Q) mutations was cloned into the Xho1 site of the Mo.PrP.Xho plasmid. The resulting Mo.PrP-tauK274/281Q (tauKQ) transgene was microinjected into fertilized mouse oocytes from the FVB/N genetic background and implanted into pseudopregnant female mice. The founder line with the highest expression of tauKQ in the FVB/N genetic background was then crossed with C57BL/6 mice purchased from Jackson Laboratory. All mice used for experiments were of mixed FVB/N and C57BL/6 genetic background. Tail DNA from offspring was genotyped by using the following primers: 5' primer GGAGTTCGAAGTGATGGAAG, 3' primer GGTTTTTGCTGGAATCCTGG. Both male and female mice were used for experiments. Mice were housed in a pathogen-free barrier facility with a 12 hour light-dark cycle and ad libitum access to food and water. All animal procedures were carried out under University of California, San Francisco, Institutional Animal Care and Use Committee-approved guidelines.

Immunoprecipitation for HPLC, electrospray ionization (ESI), and tandem MS/MS. Immunoprecipitation was done with the Pierce Direct IP Kit (Thermo Scientific), essentially as recommended by the manufacturer. Briefly, monoclonal anti-tau (ab80579, Abcam) was immobilized on agarose resin with sodium cyanoborohydride. Brain homogenates lysed in RIPA buffer (50 mM Tris, pH. 7.4, 150 mM NaCl, 1 mM EDTA, 0.5% Nonidet P-40 with histone deacetylase inhibitors (1 µM trichostatin, 5 mM nicotinamide, 1 mM phenylmethyl sulfonyl fluoride, and protease inhibitor cocktail; all from Sigma) and phosphatase inhibitor cocktail (Roche) were applied to the antibody-conjugated resin and rotated overnight at 4°C. Samples were eluted with elution buffer, pH 2.8, into collections tubes containing neutralizing Tris buffer, pH 9.5.

ESI-quadrupole time-of-flight (QqTOF) MS analyses. Bands were manually excised from the gel, destained, and dehydrated with acetonitrile. The proteins were reduced with 10 mM dithiothreitol at 60 °C for 30 min, alkylated with 100 mM iodoacetamide (37 °C, 45 min), and digested with 250 ng of sequencing-grade trypsin (Promega) at 37 °C overnight. After digestion, the proteolytic peptide mixtures were analyzed by reverse-phase nano-HPLC-ESI-MS/MS with an Eksigent nano-LC two-dimensional HPLC system (Eksigent) connected to a QqTOF QSTAR Elite mass spectrometer (Sciex).

Briefly, peptides were applied to a guard column (Dionex) and washed with the aqueous loading solvent (2% solvent B in A, flow rate: 20 µl/min) for 10 min. The samples were transferred to an analytical C18-nanocapillary HPLC column (Dionex) and eluted for 85 min with a linear gradient of 2–80% solvent B in A at a flow rate of 300 nl/min for most samples. Solvent A consisted of 2% acetonitrile and 98% 0.1% formic acid (v/v) in water. Solvent B consisted of 98% acetonitrile and 2% 0.1% formic acid (v/v) in water. Mass spectra (ESI-MS) and tandem mass spectra (ESI-MS/MS) were recorded in positive-ion mode with a resolution of 12,000–15,000 FWHM.

For collision-induced dissociation MS/MS, the mass window for precursor ion selection of the quadrupole mass analyzer was set to ±1 *m/z*. The synthetic acetylated peptide IPAKacTPPAPK (ThermoFisher Scientific/Pierce Biotechnology) for mass spectrometric comparison was analyzed by reverse-phase HPLC-ESI-MS/MS with an Eksigent Ultra Plus nano-LC two-dimensional HPLC system connected to a quadrupole time-of-flight TripleTOF 5600 mass spectrometer (Sciex) (Shilling et al., 2012). Databases were searched with Protein Pilot Software 4.5 revision 1656 (Sciex) and the Paragon Algorithm 4.5.0.0.1654 (Sciex) (Shilov et al., 2007) or an in-house Mascot server version 2.3.02 (Perkins et al., 1999). For manual inspection of peptides containing posttranslational modifications, we adapted published criteria.

Cell culture and transfection. HeLa cells in Dulbecco's modified Eagle's medium supplemented with 10% fetal bovine serum, 100 U/ml penicillin, and 100 μg/ml streptomycin were grown at 37 ℃ in 5% CO_2. Primary cultures were established from hippocampi of Sprague-Dawley rat pups (Charles River Laboratories) on postnatal day 0 or 1. Purified cells (50,000 per 300 μl of neurobasal medium supplemented with B27; Life Technologies) were plated on poly-L-lysine-coated, glass-bottom 35-mm dishes (MatTek). After cells had attached, the medium was replaced. At 6 or 7 DIV, the cells were transfected with Lipofectamine 2000 (Life Technologies) and DNA plasmids mixed 2:1 in OPTI-MEM (Life Technologies). After 30 min, the transfection medium (neurobasal medium with kyneurenic acid) was replaced with conditioned neurobasal medium supplemented with B27.

Immunostaining and confocal imaging. Mice were transcardially perfused with 0.9% saline, and the brains were fixed in 4% paraformaldehyde in PBS for 48 h and then incubated in 30% sucrose in PBS. For antigen retrieval, coronal brain sections 30 μm thick were cut with microtome and incubated in 10 mM citric acid at 90 ℃ for 20 min. Floating brain

sections were permeabilized and blocked with PBS containing 0.3% Triton X-100 and 10% normal goat serum (PBST) at room temperature for 1 h. Sections were incubated first with antibodies against AnkG (N106/36, NeuroMab) and βIV-spectrin (gift from Dr. Matthew N. Rasband, Baylor College of Medicine) at 4 ℃ overnight and then with Alex Fluor 488- and 555-conjugated anti-mouse and anti-rabbit antibodies (Life Technologies) at room temperature for 1 h. Immunostaining with human brains was performed as described previously (Grinberg et al., 2013). Briefly, cases were selected from the Neurodegenerative Disease Brain Bank (NDBB) at the University of California, San Francisco. 8 μm-thick sections were cut from paraffin blocks and mounted on glass slides. Immunoperoxidase staining was performed using an avidin-biotin complex detection system (Vectastain ABC kit; Vector Laboratories). Slides were pretreated for antigen retrieval by immersion in 10 mM citric acid at 121 ℃ for 5 min. The primary antibody mAb359 (Grinberg et al., 2013) was incubated overnight at 4 ℃ and biotinylated secondary antibody (Vector Laboratories) was incubated at room temperature for 1 h. Slides were incubated in Avidin/Biotinylated enzyme Complex (ABC) at room temperature for 1 h followed by exposure to 3,3'-diaminobenzidine (DAB) substrate (Vector Laboratories). For immunofluorescence, after antigen retrieval and blocking with 0.1% Sudan Black solution, the primary antibodies mAb359 (Grinberg et al., 2013), CP-13 (gift from Dr. Peter Davies, Feinstein Institute for Medical Research), and AnkG (N106/36, NeuroMab) were incubated overnight at 4 ℃. The secondary antibodies DyLight 488 and DyLight 549-conjugated anti-mouse and anti-rabbit antibodies were incubated at room temperature for 1 h. AIS Images were acquired with a Nikon Ti-E spinning-disk confocal microscope and a 60X oil objective. Seven serial optical sections (0.5 μm steps) were projected into a single image to visualize the AIS. ImageJ software (NIH) was used to analyze the intensity and length of the AIS.

MT-binding assay. MT binding assays in HeLa cells were performed as described (Lu and

Kosik, 2001) with modifications. DNA plasmids of mApple-mutant tau and GFP-WT tau were co-transfected into HeLa cells. To assess the intracellular distribution of WT and mutant tau, HeLa cells at 37 ℃ in 5% CO_2 were examined with a Nikon Ti-E spinning-disk confocal microscope and a 60X oil objective 24–48 h after transfection. After conversion of fluorescent RGB images into binary images, ImageJ (NIH) was used to subtract a binary image of WT tau from that of mutant tau. Cytoplasmic tau signals after the image subtraction were calculated as the MT-unbound tau index.

Measuring MT dynamics. HeLa cells were co-transfected with GFP-EB1 and mApple-tau, and primary rat hippocampal neurons at DIV 6–7 were co-transfected with GFP-EB3 and mApple-tau; the cells were imaged at 37 ℃ in 5% CO_2 24 h after transfection. Live time-lapse imaging was performed every second for 60 sec with a Nikon Ti-E spinning disk confocal microscope and a 60X oil objective. Movement of GFP-EB1 and GFP-EB3 comets were analyzed with the Matlab software package plusTipTracker (Applegate et al., 2009).

Fluorescence recovery after photobleaching (FRAP). Primary rat hippocampal neurons at DIV 6–7 were co-transfected with GFP-tubulin and mApple-tau, and imaged 24 h after transfection. Before imaging, the AIS was immunolabeled with an antibody against the extracellular domain of neurofascin (A12/18, NeuroMab) at 37 ℃ for 5 min. After brief rinses with Neurobasal A media, Alexa Fluor 647 anti-mouse secondary antibody was applied at 37 ℃ for 5 min. For FRAP experiments, we used a Nikon Ti wide-field microscope and a 100X oil objective to examine cells at 37 ℃ in 5% CO_2. An ROI (~5 μm) for photobleaching was drawn in the center of the AIS, as judged from anti-neurofascin staining. GFP-tubulin was bleached with a 473-nm laser and fluorescence recovery was monitored with a 488-nm laser. Time-lapse images were taken every second for 60 sec. Images in which photobleaching reduced fluorescence intensity by more than 70% were analyzed. The fluorescence signal was background subtracted and quantified with ImageJ (NIH).

Photoconversion. Time-lapse live imaging during photoconversion was performed as described (Li et al., 2011) using photoconvertible mEOS2-tau. Primary rat hippocampal neurons at DIV 6–7 were transfected with mEOS2-tau and imaged 48–72 h later with a Nikon Ti-E spinning disk confocal microscope at 37 ℃ with 5% CO_2. A ~30-μm portion of an axon segment ~30 μm from the cell body was subjected to photoconversion with a 405-nm laser (two to three 300-ms exposures), and red fluorescence images were acquired every 30 sec for 30 min. Using ImageJ (NIH), changes in red fluorescence intensity was analyzed in both the cell body and a distal axon ~30 μm away from the photoconversion site. Changes in red fluorescence intensity were normalized to the initial red fluorescence intensity from the photoconversion site right after photoconversion.

Western blot. Human brain tissues were lysed in RIPA buffer (50 mM Tris, pH. 7.4, 150 mM NaCl, 1 mM EDTA, 0.5% Nonidet P-40) with histone deacetylase inhibitors (1 μM trichostatin, 5 mM nicotinamide; both from Sigma), 1 mM phenylmethyl sulfonyl fluoride (Sigma), phosphatase inhibitor cocktail (Roche), and protease inhibitor cocktail (Sigma). Lysates were sonicated and centrifuged at 170,000 *g* at 4 ℃ for 15 min and at 18,000 *g* at 4 ℃ for 10 min. Supernatants were collected, and protein concentrations were measured by bicinchoninic acid assay (Pierce). Proteins were resolved on 4–12% SDS-PAGE and transferred to nitrocellulose membranes. After blocking with nonfat dry milk, the membranes were probed at 4 ℃ overnight with primary antibodies: rabbit monoclonal mAb359 (Grinberg et al., 2013), mouse monoclonal anti-AnkG (N106/20, NeuroMab), rabbit polyclonal anti-βIV-spectrin (gift from Dr. Matthew N. Rasband, Baylor College of Medicine), mouse monoclonal Tau5 (AHB0042, Life Technologies), and mouse monoclonal anti-GAPDH (MAB374, Millipore). The membranes were then incubated with HRP-conjugated secondary antibodies at room temperature for 1 h. Immunoblots were visualized by enhanced chemiluminescence (Thermo Scientific) and quantified by ImageJ software (NIH).

Differentiation of human iPSCs into neurons. The differentiation protocol of human induced pluripotent stem cells (iPSCs) from Zhang et al. (2013) was adapted for expression of a single transcription factor neurogenin-2 (NGN2) that coverts iPS cells into homogenous glutamatergic neurons. Instead of lentiviral delivery of tetracyclin-induced expression of NGN2 construct (Zhang et al., 2013), we engineered a stable WTC11 iPSC line with single site integration of NGN2 into human genome AAVS1 locus by TALENs technique and selected homozygous clonal population by puromycin. iPSCs were plated at 2×10^6 cells per well in 6-well plate in DMEM/F-12/N2/NEAA medium supplemented with BDNF (10 μg/l, INvitrogen), NT3 (10 μg/l, Invitrogen), laminin (0.2 mg/l, Invitrogen), and doxycycline (2 g/l, Clontech) for pre-differentiation for 3-5 days before re-seeding on coverslips. Pre-differentiated iPSCs were dissociated from the plate by the accutase enzyme. 5×10^5 cells per coverslip were re-seeded on matrigel-coated coverslips in neurobasal A medium supplemented with B27, glutamax, BDNF, NT3, laminin, and doxycycline (Day 0). On day 1, astrocytes were added in neurobasal medium with B27, glutamax, BDNF, NT3, laminin, doxycycline, and 2μM AraC. On day 6, doxycycline was excluded from growth medium. On day 7, serum-containing growth medium (MEM supplemented with B27, glucose, $NaHCO_3$, transferrin, L-glutamine, AraC, and FBS) was applied. In 3-4 weeks of differentation, cells became mature neurons with a single AIS and synapse formation. The iPS cell lines (GIH and 030) with V337M tau mutation were gifts from Dr. Yadong Huang (Gladstone Institutes) and Bristol Myers Squibb (BMS), respectively.

Statistical analyses. Data were analyzed with GraphPad Prism 5 and STATA12. Differences between groups were assessed with the unpaired *t* test, one-way ANOVA with post-hoc test, and mixed-model linear regression analysis as indicated. Longitudinal data were fitted with mixed-model linear regression using the xtmixed command from STATA 12. The linear relationship between two variables was analyzed by Pearson's correlation analysis

after natural log transformation.

CHAPTER 3

Acetylated tau destabilizes the cytoskeleton in the axon initial segment

and is mislocalized to the somatodendritic compartment

Acetylation at K274/281 reduces tau binding to MTs

To identify lysine residues in tau that are acetylated in human AD brains, soluble tau was extracted from AD brains with a column conjugated with the anti-tau antibody, proteolytically digested, and analyzed by HPLC-ESI-MS/MS. K274 and K281 in the MT-binding domain were acetylated (Fig. 1*A, B*). Posttranslational modifications of tau in the MT-binding domain can affect its binding affinity for MTs (Biernat et al., 1993; Wagner et al., 1996; Ballatore et al., 2007). To examine the effect of acetylation at K274/K281 on tau binding to MTs, we mutated K-to-Q to mimic acetyl-lysine or K-to-R to mimic deacetylated lysine (Hecht et al., 1995; Luo et al., 2003). To assess the binding affinity, we analyzed cells expressing mApple-WT tau and GFP-mutant tau in a competitive MT-binding assay (Lu and Kosik, 2001). In HeLa cells co-transfected with mApple-WT tau and GFP-tubulin, WT tau co-localized with MTs visualized by GFP-tubulin, indicating attachment of WT tau to MTs (Fig. 2*A*). In contrast, a tau mutant with a lower affinity for MTs exhibits more diffuse distribution than WT tau (Lu and Kosik, 2001). Thus, the unbound tau index is calculated by subtracting the fluorescence signal of mApple-WT tau from that of GFP-mutant tau. The unbound tau index for K274/281Q tau was significantly higher than WT tau, whereas K274/281R tau showed similar binding affinity as WT tau, suggesting that acetylation at K274/281 reduces tau binding to MTs. Binding of individual mutant K274Q or K281Q tau was modestly reduced. K-to-Q mutations outside the MT-binding domain (K163/174/180/190Q; 4KQ(N)) did not affect the unbound tau index, as expected (Fig. 2*B, C*). The difference in the amount of unbound cytoplasmic tau is unlikely due to different tau

expression levels, as K274/281Q and WT tau had similar levels of expression levels (Fig. 2*D*), and the unbound tau index did not correlate with tau levels (p = 0.19, Pearson correlation analysis).
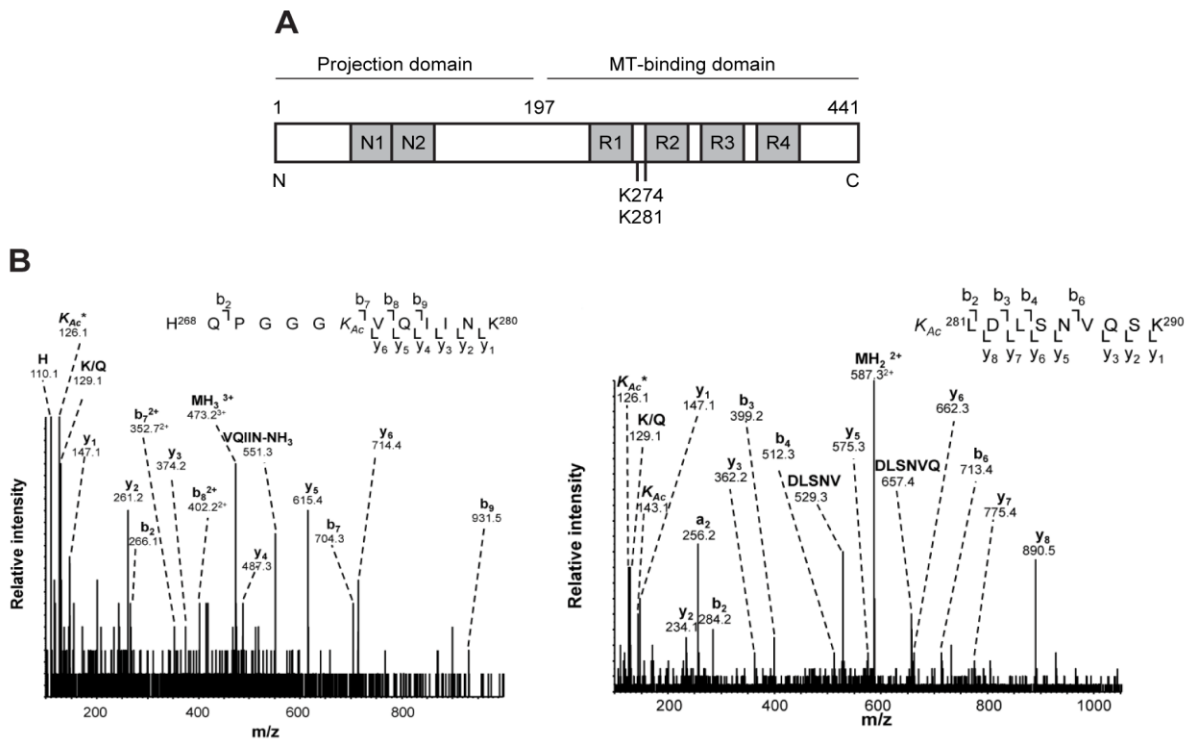
Figure 1. Ac-K274/281 tau is present in human AD brains.

(A,B) Electrospray ionization tandem mass spectrometry analysis identified two acetylated peptides, HQPGGGK$_{Ac}$VQIINK (residues 268-280) and K$_{Ac}$LDLSNVQSK (residues 281-290), from trypsin digested tau immunoprecipitated from human AD brains. (A) K274 and K281 are located in the MT-binding domain of tau. (B) The molecular ion [M+3H]$^{3+}$ at m/z 473.24 (M=1416.68) was selected for collision induced dissociation (CID) and the resulting MS/MS spectra identified ac-K274 (Mascot score 34, expectation value 0.00042). The molecular ion [M+2H]$^{2+}$ at m/z 587.32 (M=1172.62) was selected for CID and the Mascot search results identified ac-K281 (Mascot score 50, expectation value 0.000009).

K*: immonium ion marker ion at m/z 126.1 for ac-K.
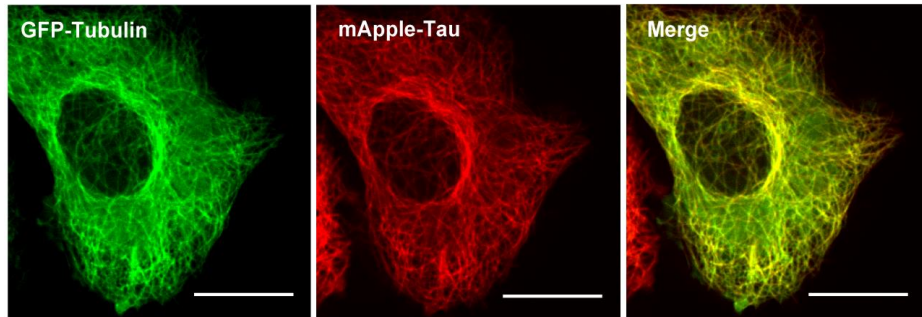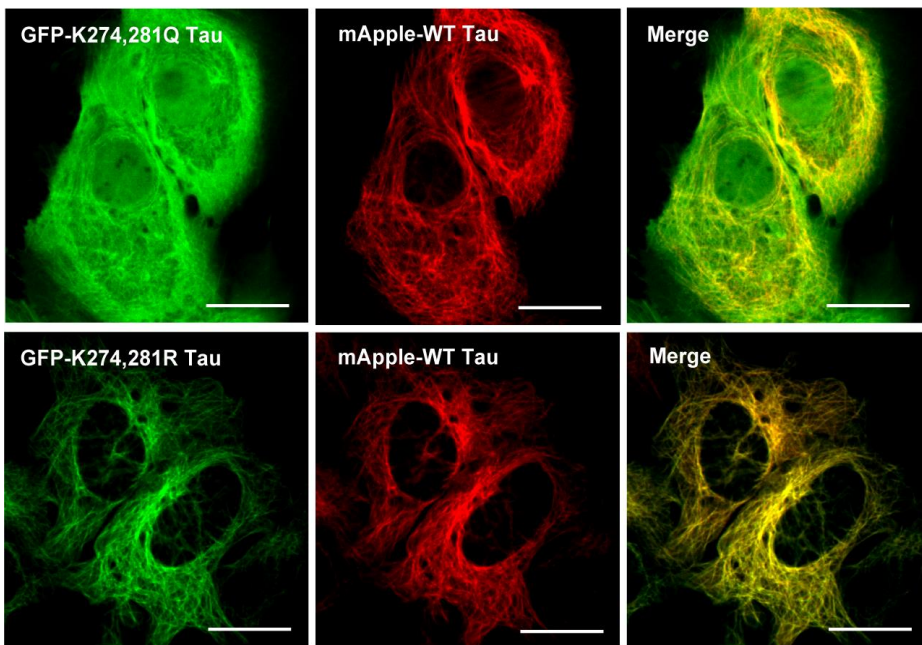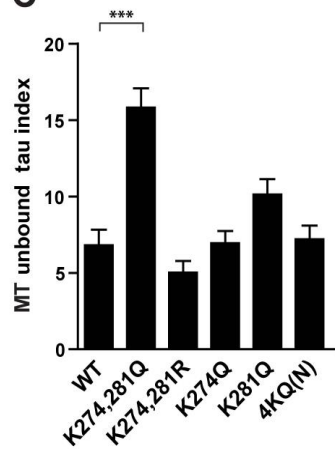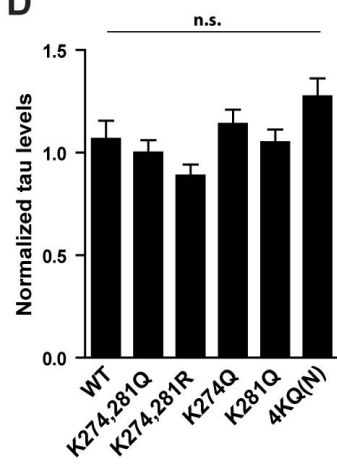
Figure 2. K274/281Q tau has reduced affinity for MTs.

(A) Representative images of co-localization of GFP-tubulin and mApple-WT tau in a HeLa cell. (B–D) MT-binding assay in HeLa cells co-transfected with GFP-mutant tau and mApple-WT tau. (B) Representative images of HeLa cells co-transfected with GFP-K274/281Q or GFP-K274/281R tau and mApple-WT tau. GFP-K274/281Q tau is distributed diffusely in the cytoplasm. mApple-WT tau appears to bind to MTs. (C,D) Quantification of MT-unbound tau and levels of tau in HeLa cells co-transfected with GFP-mutant tau and mApple-WT tau. 4KQ(N) denotes GFP-K163/174/180/190Q tau. n = 60–90 cells/group from two to three independent experiments. ***p<0.001, one-way ANOVA with Dunnett's post-hoc analyses. Values are mean ± SEM Scale bars, 10 μm.

Acetylation at K274/281 leads to hyperdynamic MTs in the AIS

Tau isoforms with different MT-binding affinities differ in their effects on the dynamic behavior of MTs (Panda et al., 2003; Bunker et al., 2004). To determine whether acetylation at K274/281 affects MT dynamics in living cells, we tracked the movement of individual MTs by using GFP-tagged ending-binding (EB) proteins that bind to MT plus-ends (Akhmanova and Steinmetz, 2008). The rates of movement were calculated in unbiased fashion with plusTipTracker, which faithfully tracks EB comets from time-lapse images of living cells (Applegate et al., 2011). HeLa cells co-transfected with GFP-EB1 and either mApple-WT or -K274/281Q tau constructs were imaged every second for 1 min (Fig. 3*A, B*). The EB1 comets moved slower in cells expressing mApple-WT tau than in mock-transfected, consistent with the notion that tau stabilizes MTs (Panda et al., 2003; Bunker et al., 2004). Cells expressing K274/281Q tau exhibited significantly faster EB1 comet movements than mock-transfected controls and those expressing WT tau (Fig. 3*C*). WT and K274/281Q tau were expressed at similar levels (Fig. 3*D*), and the rates of EB1 comet movement did not

correlate with tau levels (p = 0.87, Pearson correlation analysis). These results support that acetylation at K274/281 induces hyperdynamicity of MTs in HeLa cells.

In primary neurons, we co-transfected primary rat hippocampal neurons at 6–7 DIV with GFP-EB3 and mApple-tau constructs. EB comets were imaged 24 to 48 h after transfection, and MT dynamics were analyzed (Fig. 3*E, F*). The rate of movement was significantly higher in neurons expressing K274/281Q tau than in those expressing WT tau (Fig. 3*G*). Similarly, the levels of WT and K274/281Q tau did not differ (Fig. 3*H*), and the rates of movement of EB comets did not correlate with tau levels (p = 0.37, Pearson correlation analysis).

The stability of neuronal MTs varies depending on the cellular compartment. MTs in the AIS are highly stabilized by modifications and bundling and function as a barrier to maintain the polarized distribution of tau in axons (Nakata et al., 2011; Jones et al., 2014; Li et al., 2011). Since acetylation at K274/281 increased MT dynamics in neurons, we examined the effect of tau acetylated at K274/281 on the stability of the MTs in the AIS by FRAP. Rat hippocampal neurons at 6–7 DIV were co-transfected with GFP-tubulin and mApple-tau constructs; 24 h later, we labeled the AIS of live neurons with an antibody against the extracellular domain of neurofascin, located in the plasma membrane of the AIS (Leterrier et al., 2011). The neurofascin antibody delineated the AIS during live imaging (Fig. 4*A*), enabling us to photobleach GFP-tubulin in a segment of the AIS. Monitoring of the GFP-tubulin signal for 1 min after photobleaching showed a significantly faster fluorescence recovery rate in cells expressing K274/281Q tau than in those expressing similar levels of WT tau (Fig. 4*B, C*), consistent with destabilization of MTs in the AIS by K274/281Q tau.
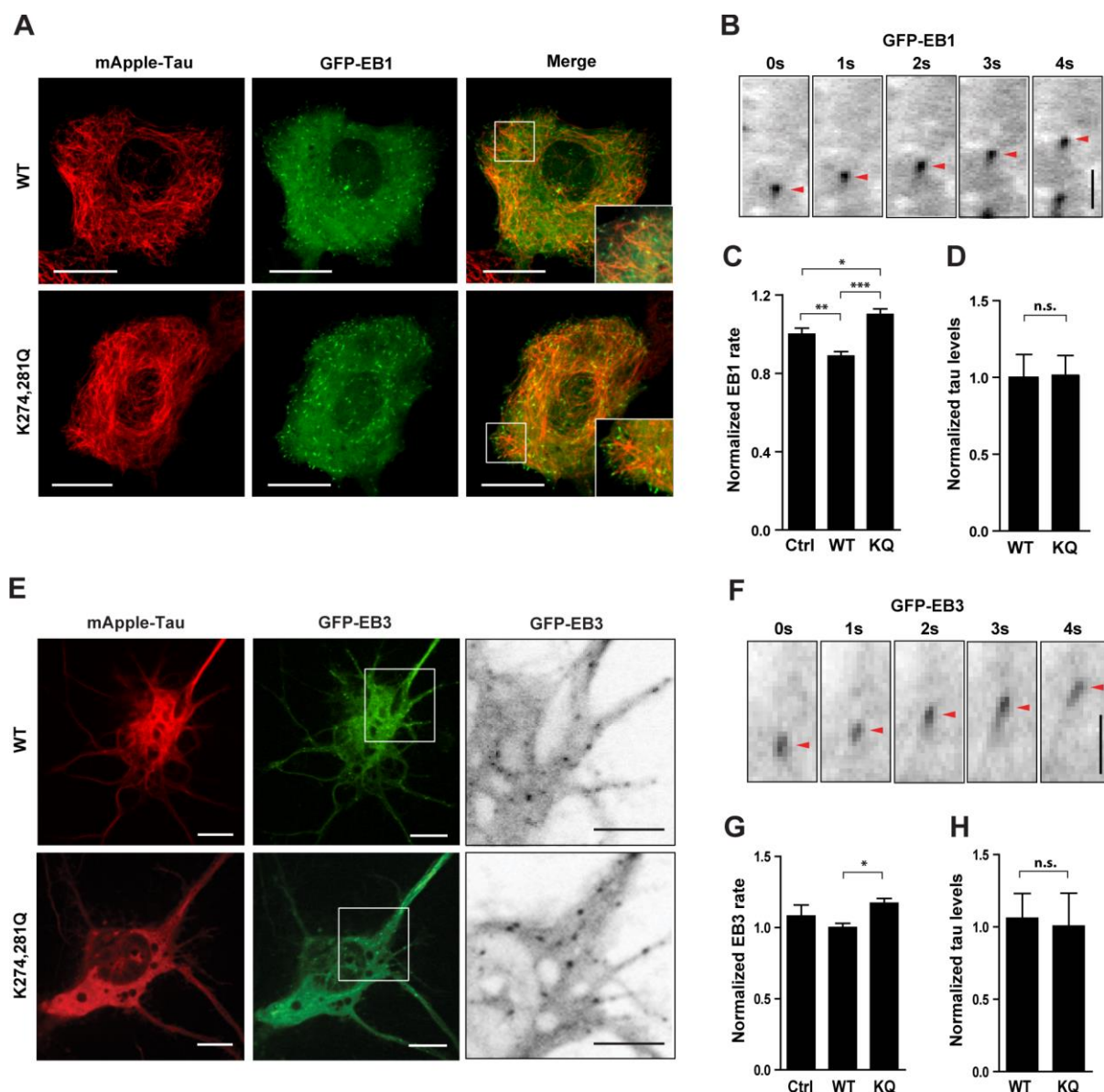
Figure 3. K274/281Q tau increases MT dynamics in HeLa cells and primary neurons.

(A–D) Measuring MT dynamics with GFP-EB1 in HeLa cells. (A) Representative images of

HeLa cells co-transfected with mApple-WT or mApple-K274/281Q tau and GFP-EB1. Insets

show labeling tips of MTs by GFP-EB1 within white boxes. Scale bars, 10 μm. (B)

Movement of a GFP-EB1 comet (arrowheads). Scale bar, 2 μm. (C,D) Quantification of the

rate of GFP-EB1 movement and tau levels in HeLa cells co-transfected with GFP-EB1 and

mApple-tau. Controls were transfected only with mApple. n = 14–16 cells/group from two independent experiments. *p < 0.05, **p < 0.01, ***p < 0.001, one-way ANOVA with Tukey's post hoc test. (E–H) Measuring MT dynamics with GFP-EB3 in rat primary neurons. (E) Representative images of HeLa cells co-transfected with mApple-WT or mApple-K274/281Q tau and GFP-EB3. Enlarged images show GFP-EB3 comets within white boxes. Scale bars, 5 μm. (F) Movement of an individual GFP-EB3 comet (arrowheads) Scale bar, 2 μm. (G,H) Quantification of GFP-EB3 movement rate and tau levels in rat primary neurons co-transfected with GFP-EB3 and mApple-tau. n = 9–13 cells/group from two independent experiments. *p < 0.05, one-way ANOVA with Tukey's post hoc test. Values are mean ± SEM.
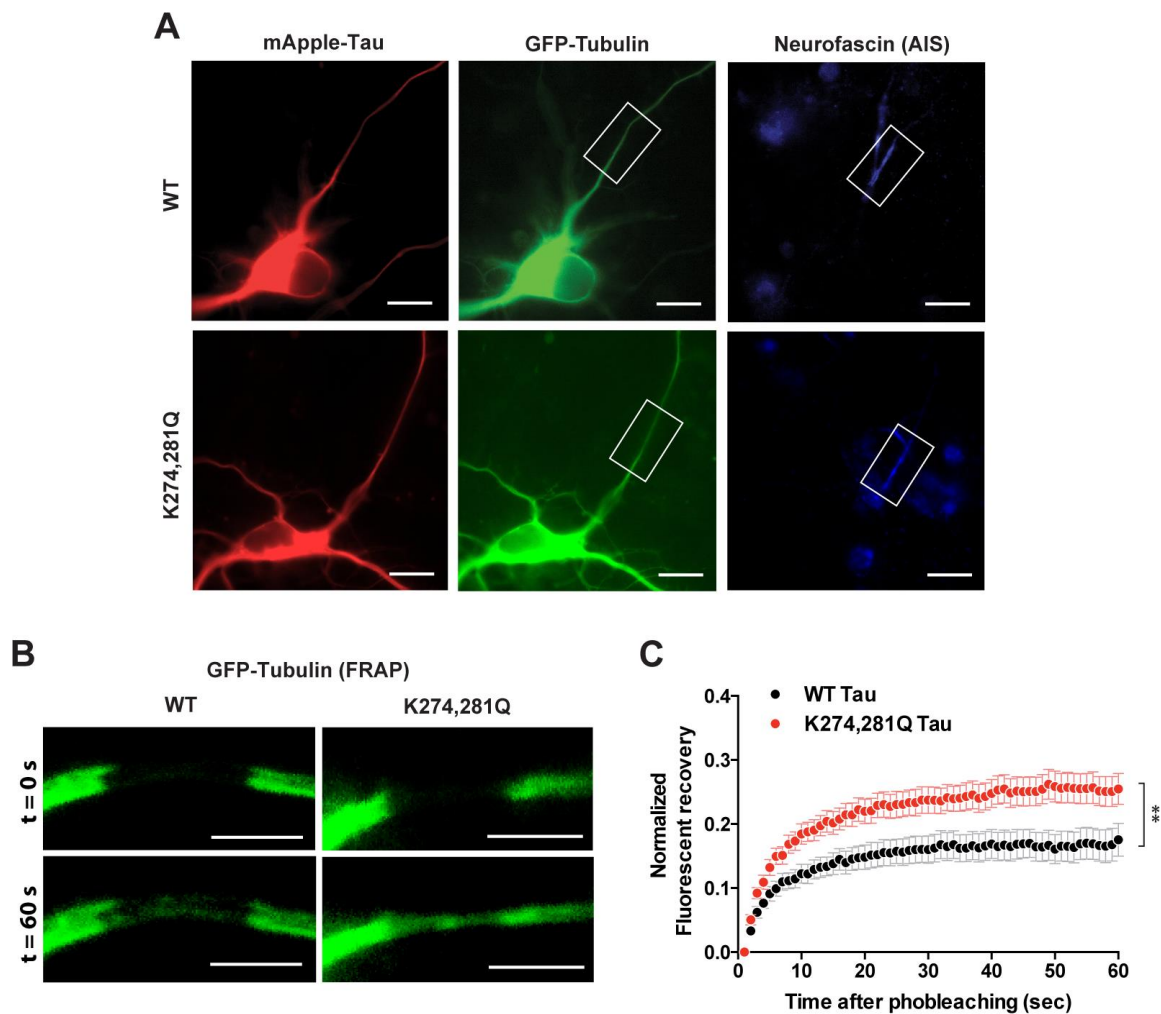
Figure 4. K274/281Q tau increases tubulin dynamics in the AIS.

(A) Representative images of a rat primary neuron co-transfected with mApple-WT or mApple-K274/281Q tau and GFP-tubulin. White boxes indicate the portion of the AIS (revealed by anti-neurofascin) where GFP-tubulin was photobleached. (B) Representative images of photobleaching and fluorescence recovery of GFP-tubulin in a ~5-μm portion of the AIS in rat primary neurons transfected with mApple-WT or mApple-K274/281Q tau. (C) Quantification of FRAP of GFP-tubulin in the AIS of rat primary neurons co-transfected with mApple-WT or mApple-K274/281Q tau and GFP-tubulin. n = 25–26 cells/group from three independent experiments. **p<0.01, mixed model linear regression analysis. Values are mean ± SEM. Scale bars, 5 μm.

Neuronal expression of K274/281Q tau reduces levels of AIS cytoskeleton *in vivo*

Next, we examined whether tau acetylation at K274/281 destabilizes the AIS cytoskeleton *in vivo*. Transgenic mice were generated to express K274/281Q human tau (2N4R) in the brain under the prion promoter (Fig. 5*A*). Since MTs in the AIS are connected to submembranous cytoskeletal proteins in the AIS such as βIV-spectrin and AnkG (Leterrier et al., 2011; Jones et al., 2014), we suspected that changes in stability of one component of the AIS cytoskeleton could alter the integrity of other components of the AIS cytoskeleton. We therefore characterized βIV-spectrin and AnkG by immunohistochemistry in the transgenic mice expressing K274/281Q tau (tauKQ mice). Fluorescence intensities of βIV-spectrin and AnkG staining were analyzed in the somatosensory cortex. Indeed, there was a significant decrease in βIV-spectrin and AnkG present at the AIS in tauKQ mice compared to nontransgenic controls, suggesting that acetylation at K274/281 can lead to destabilization of the AIS

cytoskeleton *in vivo* (Fig. 5*B–D*). The length of the AIS cytoskeleton, which can be modulated by external stimuli (Kuba et al., 2010; Grubb and Burrone, 2010), did not differ in tauKQ and control mice (Fig. 5*E*).
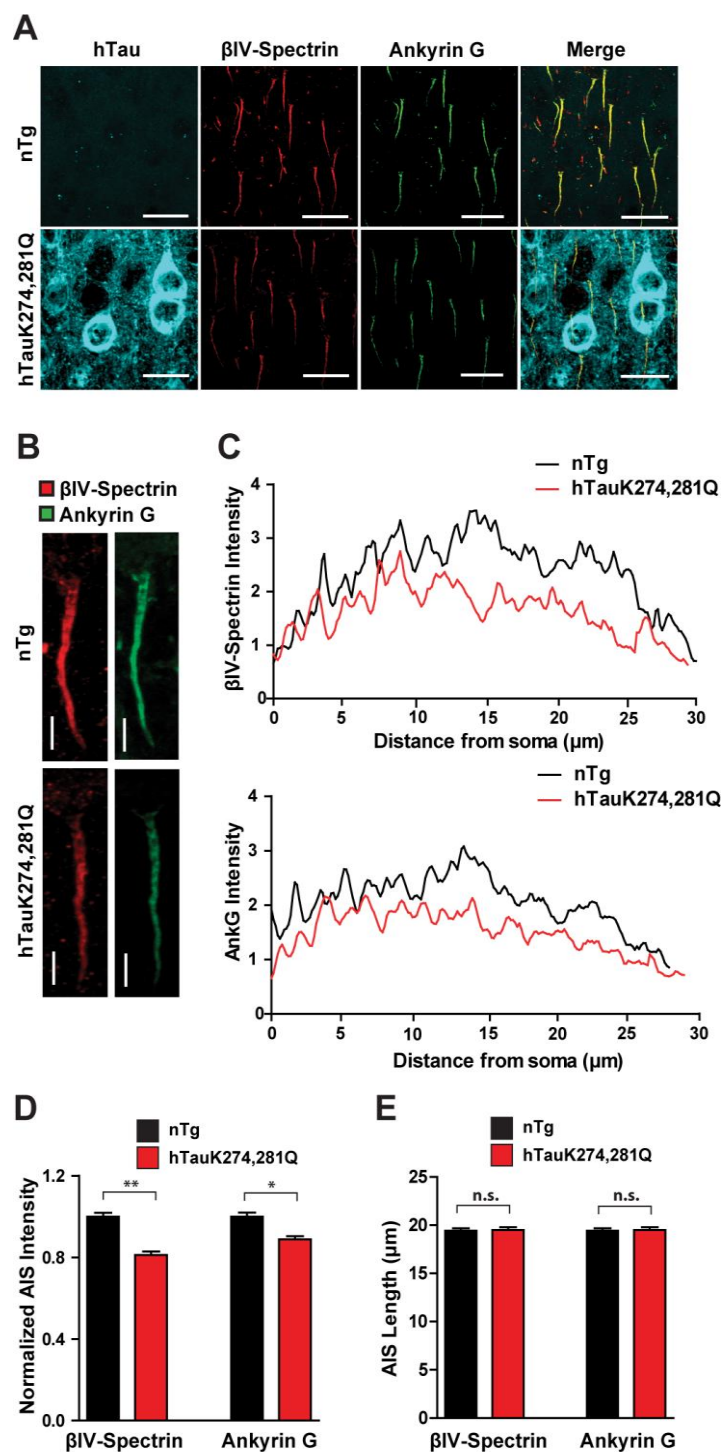
Figure 5. K274/281Q tau destabilizes AIS cytoskeleton in tauKQ mice.

(A) Representative images of hTau, βIV-spectrin, and AnkG immunostaining in somatosensory cortex of 2 month-old nontransgenic and tauKQ mice. Scale bars, 20 μm. (B,C) Representative images and fluorescent intensity profiles of βIV-spectrin and AnkG immunostaining in somatosensory cortex of 2 month-old nontransgenic and tauKQ mice. Scale bars, 5 μm. (D,E) Quantification of intensity and length of βIV-spectrin and AnkG immunostaining in the somatosensory cortex of 2 month-old nontransgenic and tauKQ mice. n = 119–132 cells from 6 mice/group. *p < 0.05, **p < 0.01, mixed-model linear regression analyses. Values are mean ± SEM.

AIS cytoskeletal proteins are downregulated in human AD brains

Acetyl-K274/281 tau was detected from human AD brain by mass-spectrometry (Tracy et al., unpublished observations). Acetyl-K274 tau detected with mAb359 was highly enriched in intraneuronal tau inclusions in human tauopathy brains (Fig. 6*A-C*; Grinberg et al., 2013). Acetyl-K274 tau was localized in the cytoplasm of neurons of FTDP-17 patients (Fig. 6*A*) and also in the corticobasal bodies of patients with A152T mutation (Fig. 6*B*), which is linked with increased risk of AD and progressive supranuclear palsy (PSP) (Coppola et al., 2012). In AD patients, acetyl-K274 tau was localized in the neurofibrillary tangles (Fig. 6*C*). Interestingly, unlike phosphorylated tau, which was localized in the soma and processes, mAb359-positive signal appeared highly enriched in the soma. Processes, including axons where tau is normally expressed, were largely devoid of mAb359-positive acetyl-K274 tau (Fig. 6*D*). Interestingly, levels of AnkG in the AIS appeared to be reduced in AD brains (Fig. 6*E*). Semi-quantitative western blot confirmed that the levels of acetyl-K274 tau were higher, whereas those of AnkG and βIV-spectrin were lower, at late Braak stages than at early Braak stages of AD patients (Fig. 6*F, G*; Table 1). Moreover, levels of AnkG and βIV-spectrin

correlated negatively with those of acetyl-K274 tau (Fig. 6*H*), raising the possibility that increased levels of acetyl-K274 tau in AD brains could downregulate AIS cytoskeletal proteins.

Table 1

AD human brain samples from superior temporal gyrus

Case number	Braak	Gender	Age	Plaque load (# plaques/mm2/temporal gyrus)
2010	0	M	70	0
1248	0	M	83	0
1036	0	M	93	0
1248	0	M	83	0
1004	1	M	75	0
1180	1	F	73	0
1028	1	M	88	0
1279	2	M	71	0
546	2	F	80	0
1040	2	F	74	0
776	2	M	95	0
1088	2	M	73	0
625	5	F	102	0.4
399	5	M	96	9.7
247	5	F	73	8.4
326	5	M	88	25.2
675	5	F	85	18.4
9	5	F	88	15.6
607	6	F	103	7.6
611	6	F	87	3.04
1203	6	F	93	6.4
736	6	F	94	9.2
649	6	F	84	10.8
992	6	F	88	6
505	6	F	94	12
350	6	F	88	13.2
697	6	F	100	9.2
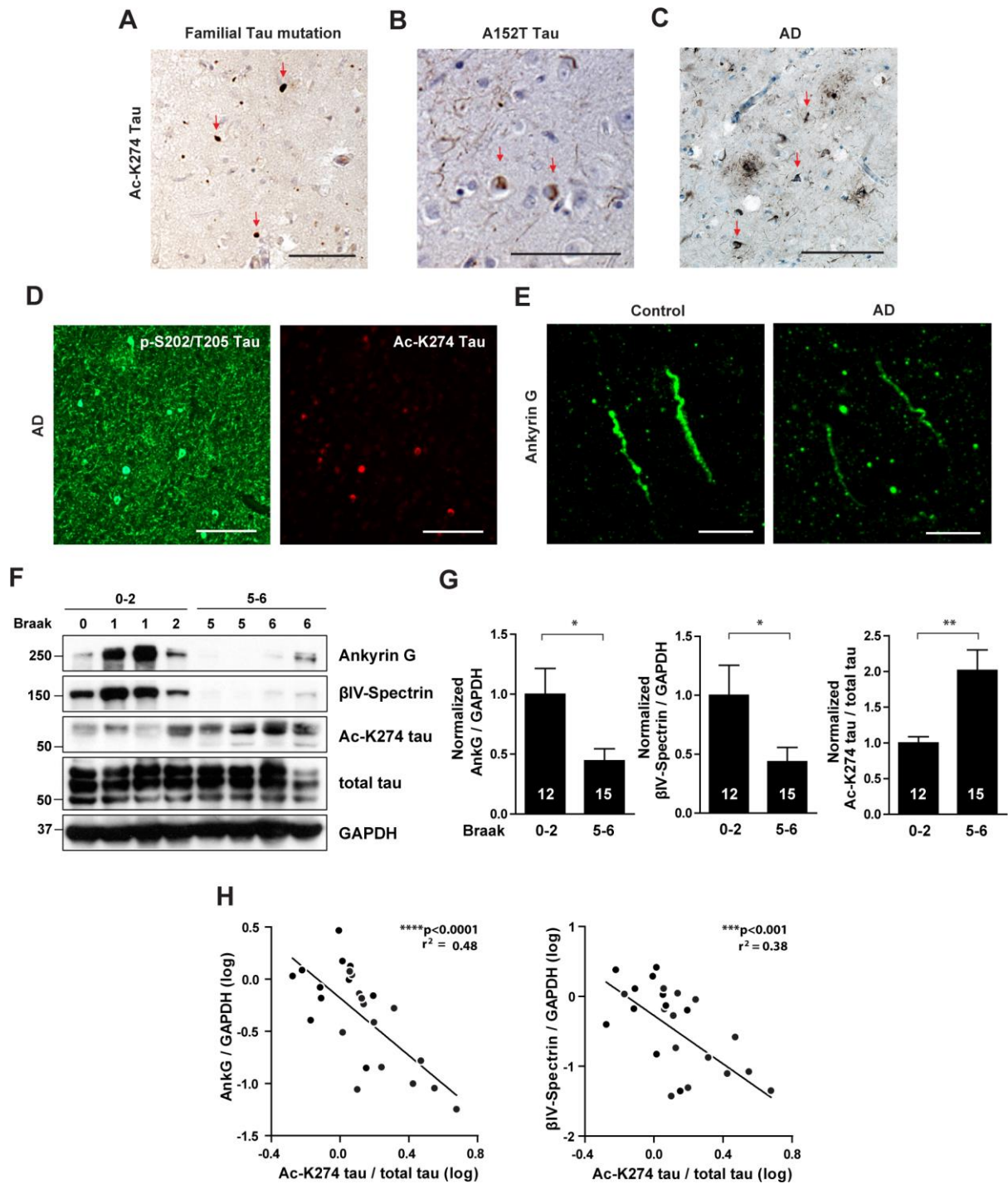
Figure 6.   Levels of AIS cytoskeletal proteins are downregulated in human AD brains and correlate negatively with ac-K274 tau levels.

(A-C) Representative images of ac-K274 tau immunostaining in the inferior temporal cortex of human tauopathy brains. Scale bars, 50 μm. (A) Cytoplasmic tau inclusions (arrows) in the

brain of FTDP-17 patients. (B) Corticobasal bodies (arrows) in patients with A152T tau mutation. (C) Neurofibrillary tangles (arrows) in AD brains. (D) p-S202/T205 and ac-K274 tau immunostaining in AD brains. Scale bars, 50 μm. (E–H) Measuring AIS cytoskeletal proteins and ac-K274 tau in human AD brains. (E) Representative images of AnkG immunostaining in human control and AD brains. Scale bars, 10 μm. (F,G) Representative western blots and quantification of levels of AnkG, βIV-spectrin, and ac-K274 tau in human AD brains. n = 12–15 samples/group. *p < 0.05, **p < 0.01, unpaired *t* test. (H) Correlation analyses between AnkG or βIV-spectrin and ac-K274 tau. Pearson correlation analyses after natural log transformation. Values are mean ± SEM (G).

Acetylation at K274/K281 leads to the somatodendritic mislocalization of tau, which can be rescued by EpoD

Since the AIS is implicated in restricting tau distribution in the axon (Li et al., 2011), we suspected that acetylation at K274/281 that weakens the AIS barrier could lead to mislocalization of axonal tau. Photoconvertible tau constructs were used to monitor the movement of tau in rat hippocampal neurons. At DIV 6–8, the cells were transfected with mEOS2-tau constructs that turns red upon UV illumination. Tau in an AIS segment ~30 μm away from the cell body was targeted for photoconversion, and influx of tau into the somatodendritic compartment was monitored (Fig. 7*A*). As judged from the increase in fluorescence intensity, the influx was much greater with K274/281Q tau than WT tau or K274/281R tau (Fig. 7*B, C*). The higher influx rate suggests that acetylation at K274/281 enabled tau to bypass the sorting barrier in the AIS. In the distal axons, cells expressing both constructs showed similar time-dependent increase in fluorescence intensity, suggesting that both WT and K274/281Q tau can freely in the absence of AIS barrier (Fig. 7*D*).

To test whether stabilization of MTs could restore the AIS barrier function and prevent

mislocalization of acetylated tau, we treated the neurons expressing K274/281Q tau with a low dose of epothilone D (EpoD), an MT stabilizer, to reduce MT dynamics (Zhang et al., 2012; Barten et al., 2012). Treatment with EpoD prevented the influx of axonal K274/281Q tau into the somatodendritic compartment (Fig. 7*B, C*). EpoD also modestly slowed down the movement of K274/281Q tau to the distal portion of axon (Fig. 7*D*). These findings support the importance of MT stability in controlling axonal sorting of tau.

Mislocalization of tau occurs early in disease progression, and dendritic tau contributes to the pathogenesis of neurodegenerative diseases (Ittner and Gotz, 2011; Zempel and Mandelkow, 2014). We hypothesized that prevention of tau mislocalization by stabilization of MTs could ultimately result in the amelioration of tau pathology. To test whether stabilization of MTs would reduce acetylated tau-driven pathology, we conducted the immunohistochemistry with the MC1 antibody targeting the tau protein with pathological conformation (Jicha et al., 1997) in the K274/281Q tau-expressing transgenic mice with weekly injections of 1mg/kg EpoD for 3 months. The levels of tau with pathological conformation recognized by the MC1 antibody in cortex were reduced in the transgenic mice with EpoD treatment compared to vehicle-treated transgenic mice (Fig.8*A, B*).
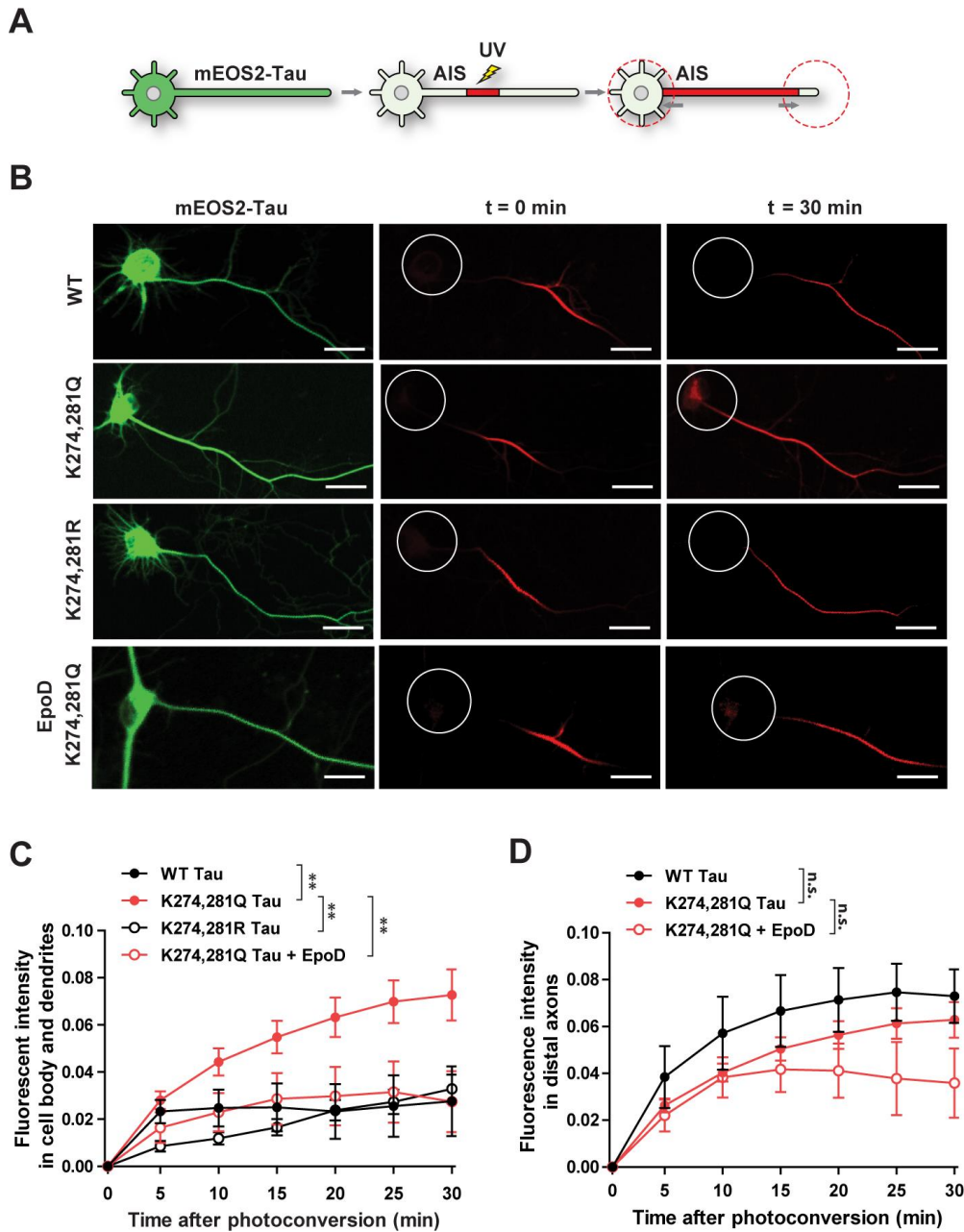
Figure 7. Stabilization of MTs reduces somatodendritic mislocalization of K274/281Q tau.

(A–D) Photoconversion of mEOS2-tau and its movement in rat primary neurons. (A) Schematic diagram of photoconversion of mEOS2-tau in the AIS and monitoring its movement toward somatodendritic compartment and distal axon. (B) Time-lapse live images of mEOS2-WT, mEOS2-K274/281Q, and mEOS2-K274/281R tau before and after

37

photoconversion in an axon segment of ~30 μm next to the AIS. The last row represents

photoconversion of mEOS2-K274/281Q tau after EpoD treatment (20 nM). Circles indicate

the somatodendritic compartment. Scale bars, 10 μm. (C,D) Quantification of fluorescent

intensity in the somatodendritic compartment (C) and distal axon (D) for 30 min after

photoconversion of mEOS2-tau in rat primary neurons. n = 8–21 cells/group from three to

nine independent experiments. *p < 0.05, **p < 0.01, mixed model linear regression analyses.

Values are mean ± SEM.
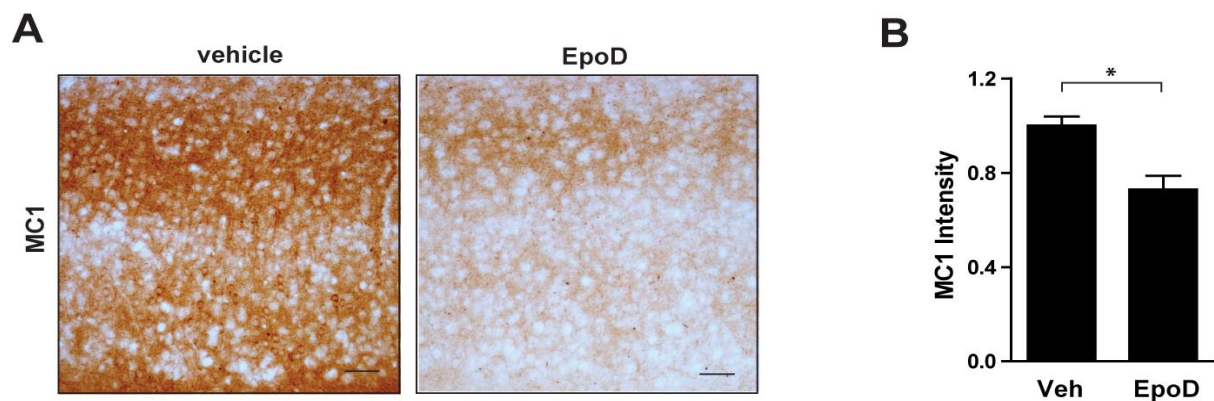
Figure 8. Stabilization of MTs reduces tau pathology in tauKQ mice.

(A,B) Representative image and quantification of MC1 immunostaining in the somatosensory

cortex of tauKQ mice treated with EpoD (1 mg/kg) or vehicle. n = 18 sections from 6

mice/group. *p < 0.05, mixed-model linear regression analyses. Values are mean ± SEM.

Scale bars, 100 μm.

CHAPTER 4

Characterization of the AIS in human iPSC-derived neurons

Characterization of the AIS in human iPSC-derived neurons with V337M tau mutation

Expression of a single transcription factor NGN2 coverts iPS cells into homogeneous glutamatergic neurons (Zhang et al., 2013). We engineered a stable iPS cell line with single site integration of NGN2 into human genome AAVS1 locus by TALENs technique. The iPS cells were pre-differentiated with tetracycline-induced expression of NGN2 and re-seeded on coverslips. Serial growth medium changes with addition of glia, addition of serum, and removal of doxycycline led to differentiation into morphologically and functionally mature neurons in 3-4 weeks (Fig. 9*A*). To confirm the polarization of neurons, immunostaining with axonal and dendritic markers – AnkG and MAP2, respectively – was performed. iPSC-derived neurons after 5-week differentiation possessed a single axon labeled with AnkG at the AIS and multiple dendrites labeled with MAP2, which is absent in axons, suggesting robust polarization into asymmetric structures which are a key characteristics of healthy neurons (Fig. 9*B*). Interestingly, differentiation with astrocytes led to enlarged soma with multiple AIS structures, indicating that astrocytes may play a critical role in establishment of neuronal polarity (Fig. 9*C*). The differentiated human neurons exhibited clustering of voltage-gated sodium channels in the AIS which are essential for generation of action potentials (Fig. 9*D*).

To determine whether pathogenic tau alters AIS characteristics in human iPSC-derived neurons, we analyzed the AIS location and length of human neurons derived from patients with FTDP-17 tau mutation (V337M). AnkG immunostaining in two independent lines with V337 mutation (030 and GIH) showed that starting point of the AIS in V337M tau neurons was shifted distally in axons compared to WT tau neurons. The AIS length was unaltered in

V337M tau neurons (Fig. 10*A, B*). To examine dynamic features of the AIS in human neurons in response to increased neuronal activity, we treated them with 10mM KCl for 32 h. Unlike in rodent neuronal cultures where relocation of the AIS occurs (Grubb and Burrone, 2010), human neurons significantly shortened their AIS length upon stimulation with KCl. This unique phenomenon of AIS plasticity in human neurons was impaired in V337M tau neurons. V337M tau neurons failed to reduce the AIS length in response to KCl, but they rather appeared to change their AIS location toward the soma (Fig. 10*A, B*).

Characterization of the AIS in human iPSC-derived neurons with tau knockdown

Recent studies have demonstrated that tau regulates neuronal excitability. Genetic reduction of tau attenuates network hyperexcitability (Roberson et al., 2011; Holth et al., 2013; DeVos et al., 2013). Although the roles of tau in synaptic plasticity have been studied to explain tau's role in activity modulation, it is still unknown whether tau can affect AIS plasticity which can change the overall excitability of a neuron. To determine whether tau plays a role in establishing static and dynamic features of the AIS, we performed tau knockdown with RNA interference and analyzed the AIS location and length. Application of 1μM tau siRNA for one week in human iPS neuronal cultures was sufficient to lead to significant reduction in levels of tau protein (Fig. 11*A*). AnkG immunostaining revealed that the AIS length was increased in human neurons with tau knockdown. The AIS starting location was unchanged with tau knockdown. The extent of reduction of the AIS length in response to KCl appeared to be larger in human neurons with tau knockdown (Fig. 11*B, C*). Although these data are preliminary, they suggest a restrictive role of tau in determining the AIS length in both static and dynamic states.
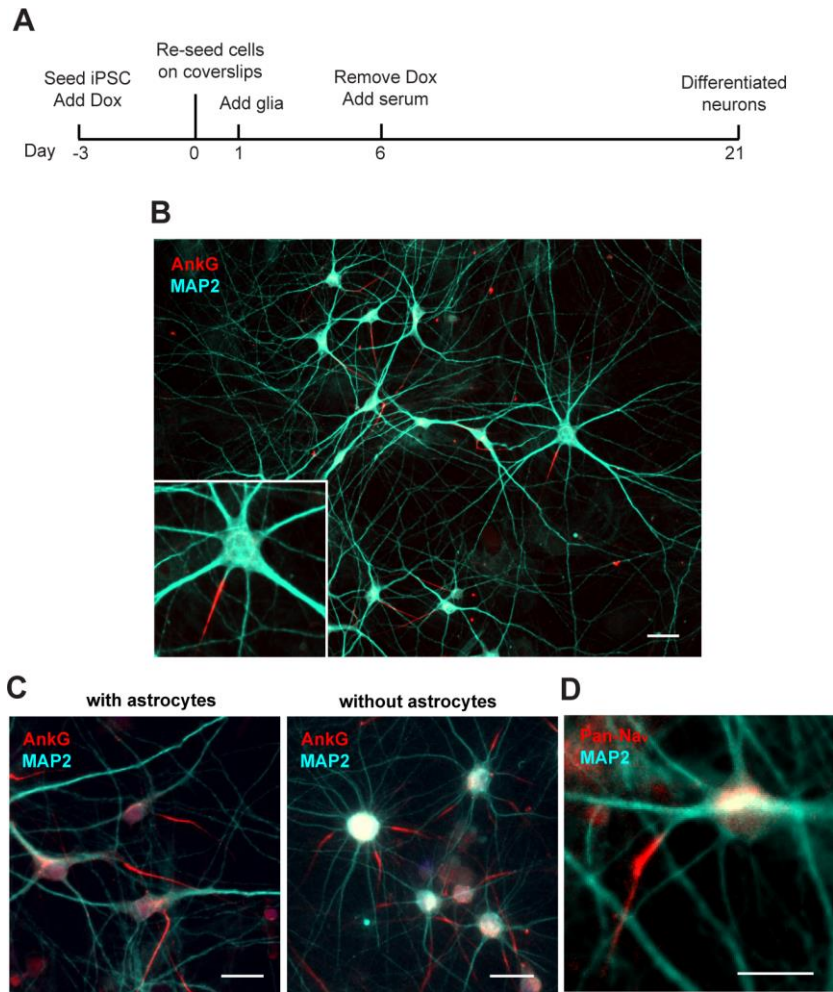
Figure 9. Differentiation of human iPSC-NGN2 stable line into neurons.

(A) Schematic describing iPSC differentiation protocol into neurons. Inducible expression of NGN2 by doxycycline followed by incubation in serum-containing medium led to differentiation into neurons in 3 weeks. (B) AnkG and MAP2 immunostaining of polarized iPSC-derived neurons after 5 weeks of differentiation. (C) Representative images of AnkG and MAP2 immunostaining of iPSC-derived neurons with and without astrocytes after 5 weeks of differentiation. (D) Pan-Na$_v$ and MAP2 immunostaining of polarized iPSC-derived neurons after 5 weeks of differentiation. Scale bars, 20 μm.
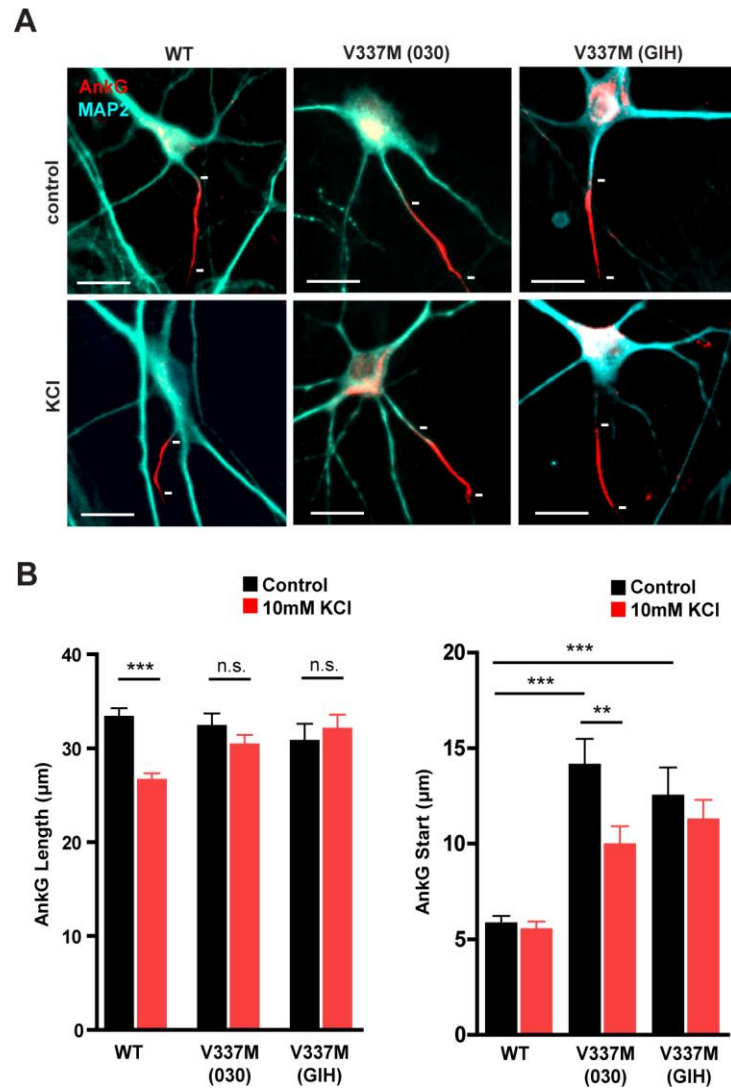
Figure 10. Activity-dependent AIS plasticity in human iPSC-derived neurons and its impairment in human iPSC-derived neurons with V337M tau mutation.

(A) Representative images of AnkG and MAP2 immunostaining of WT and two V337M tau iPSC lines with either 10mM NaCl (control) or 10mM KCl treatment for 32 h after 5-6 weeks of differentiation. Short white lines indicate start and end locations of the AIS. Scale bars, 20 μm. (B) Quantification of length and start location of AnkG immunostaining of WT and two V337M tau iPSC lines with either 10mM NaCl (control) or 10mM KCl treatment for 32 h after 5-6 weeks of differentiation. n = 28-165 cells/group from 1-2 independent experiments.

**p < 0.01, ***p < 0.001, one-way ANOVA with Tukey's post hoc test. Values are mean ± SEM.
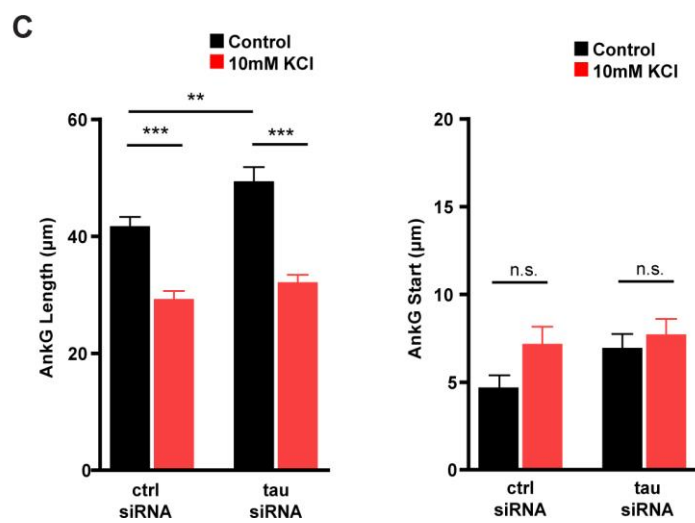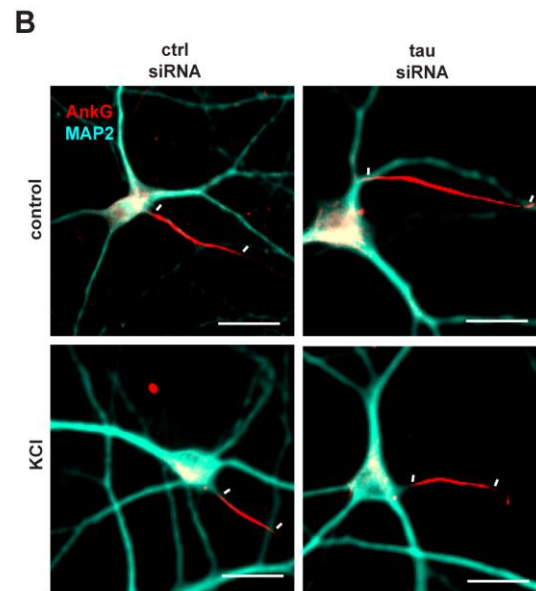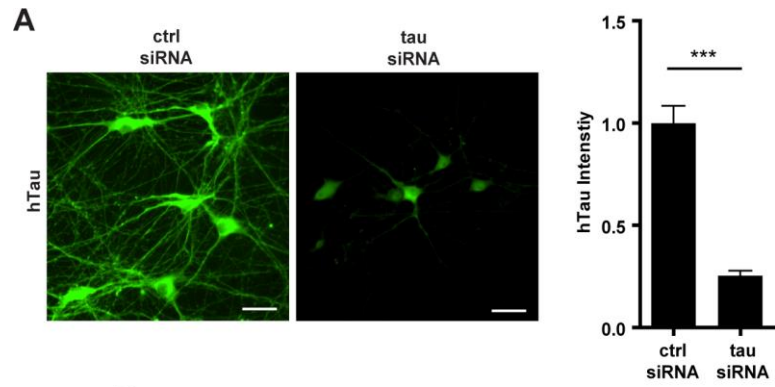
Figure 11. Activity-dependent AIS plasticity in human iPSC-derived neurons with tau knockdown.

(A) Representative images and quantification of tau knockdown by hTau immunostaining of human iPSC-derived neurons incubated with either 1μM control siRNA or 1μM tau siRNA for 1 week after 5 weeks of differentiation. Scale bars, 20 μm. ***$p < 0.001$, unpaired student t-test. (B,C) Representative images and quantification of AnkG and MAP2 immunostaining of human iPSC-derived neurons incubated with either 1μM control siRNA or 1μM tau siRNA for 1 week after 5 weeks of differentiation. Each group was treated with either 10mM NaCl (control) or 10mM KCl treatment for 32 h. Short white lines indicate start and end locations of the AIS. Scale bars, 20 μm. n = 39-48 cells/group from 1 experiment. **$p < 0.01$, ***$p < 0.001$, one-way ANOVA with Tukey's post hoc test. Values are mean ± SEM.

CHAPTER 5

Conclusion and Discussion

This study shows that AD-relevant acetylation of tau at K274 and K281 has a critical role in the somatodendritic mislocalization of tau. A mutant tau (K274/281Q) that mimics acetylation had reduced affinity for MTs and increased MT dynamics in the AIS. AIS-specific cytoskeletal proteins were downregulated in the brain both in transgenic mice expressing K274/281Q tau and in human AD patients. Destabilization of the AIS cytoskeleton resulted in mislocalization of K274/281Q tau into the somatodendritic compartment. Pharmacological stabilization of MTs prevented tau mislocalization. Our findings support aberrant tau acetylation as a novel mechanism by which pathogenic tau is mislocalized in the pathogenesis of neurodegenerative diseases. Characterization of the AIS in human iPSC-derived neurons reveals aberrant AIS location and impaired AIS plasticity in V337M tau neurons.

Pathogenic mutations increase MT turnover and perturb MT stability in transgenic mice expressing human P301S or P301L tau (Zhang et al., 2005, 2012; Barten et al., 2012). However, little is known about the underlying mechanisms. In HeLa cells and primary neurons, our current study showed that acetyl-mimicking K274/281Q tau led to elevated MT movements compared with cells expressing WT tau, suggesting MT hyperdynamicity induced by tau acetylation.

Neurons are highly polarized cells and MT dynamics in a neuron varies depending on the subcellular location (Conde and Caceres, 2009). Unlike those in dendrites and distal axons, MTs in the AIS are highly stable (Leterrier et al., 2009; Konishi and Setou 2009). Tau acetylated at K274 and K281 reduces the stability of MTs in the AIS, as measured with site-specific FRAP to monitor tubulin dynamics. Acetylated tau also destabilized the AIS

cytoskeleton *in vivo*. AnkG and βIV-spectrin are essential for AIS stability since depletion of either AnkG or βIV-spectrin dismantles the AIS (Jenkins and Bennett, 2001; Komada and Soriano, 2002; Hedstrom et al., 2008). TauKQ mice had reduced levels of the cytoskeletal proteins AnkG and βIV-spectrin in the AIS. AnkG and βIV-spectrin levels were also decreased in human AD brains, consistent with a report that the AIS filtering machinery was impaired in a mouse model of AD (Sun et al., 2014). The level of acetylated tau increases as AD pathology proceeds (Min et al., 2010) and, in particular, ac-K274 tau accumulates in human brains with tau inclusions (Fig. 6 *A-D*; Grinberg et al., 2013). In human AD brains, we found elevated levels of ac-K274 tau, which correlated negatively with the levels of AnkG and βIV-spectrin. Since the AIS cytoskeleton is critical for maintaining axonal-dendritic asymmetry (Rasband, 2010), the downregulation of AIS cytoskeletal proteins in mice and humans suggests that sorting of neuronal proteins that require polarized distribution may be impaired in AD brains with increased acetylated tau.

How does acetylated tau destabilize MTs, AnkG, and βIV-spectrin in the AIS? MTs and the submembranous cytoskeleton appear to be both physically and functionally connected. MT bundles in the AIS are densely coated with an actin-based cytoskeletal network that contains AnkG and βIV-spectrin (Jones et al., 2014). EB1 and EB3 may connect MTs to AnkG, and EB1/3 knockdown leads to downregulation of AnkG in the AIS (Leterrier et al., 2011). On the other hand, a mutation in ankyrin disrupts MT organization in *C. elegans* (Maniar et al., 2012). Tau interacts with EB1 and EB3 and augments their binding to MTs (Sayas et al., 2015). One likely mechanism could be that acetylated tau reduces EB1/3 binding to MTs, leading to destabilization of MT and downregulation of AnkG and βIV-spectrin in the AIS. Considering tau's potential role in connecting MTs and actin-based cytoskeletal networks (Farias et al., 2002), it is also possible that, independently of EB1/3, the AIS submembranous cytoskeleton might be destabilized by altered direct binding of

acetylated tau to cytoskeletal networks consisting of actin, AnkG, and βIV-spectrin. These two models are not mutually exclusive.

Our finding that MTs in the AIS are critical for axonal retention of tau is consistent with the notion that they form a retrograde barrier that keeps axonal tau from entering the somatodendritic compartment (Li et al., 2011). Acetylated tau destabilizes this MT-based barrier in the AIS and thus could enter the somatodendritic compartment. MT stabilization with EpoD restored this barrier function and prevented mislocalization of acetylated tau. Pharmacological MT stabilization reduces tau binding to MTs (Kar et al., 2003; Samsonov et al., 2004), and EpoD dissociates tau from MTs (unpublished data). Increased diffusion of MT-free tau could contribute to circumvention of the MT-based barrier in the AIS (Li et al., 2011). However, low-dose EpoD prevented acetylated tau from mislocalization – a finding that emphasizes the importance of MT stability in the barrier function for retention of axonal tau. Since the submembrane AIS cytoskeleton functions as a filter controlling cytoplasmic transport in a neuron (Song et al., 2009), reduction of AnkG and βIV-spectrin levels by acetyl-K274/281 tau might also contribute to tau mislocalization. MT stabilization with EpoD prevented tau mislocalization and thus might increase the stability of interconnected AIS submembrane cytoskeletal networks. Our findings suggest that acetylated tau has an active role in disturbing stability of MTs in the AIS, resulting in circumvention of MT-based barrier in the AIS and consequent somatodendritic mislocalization.

EpoD administration in transgenic mice expressing human P301S or P301L protects mice against MT dysfunction and AD-like pathology (Zhang et al., 2005 and 2012; Barten et al., 2012). Our transgenic mice expressing human K274/281Q Tau developed misfolded Tau recognized with MC1 antibody even in their young ages of 5 months. Intraperitoneal injection of 1mg/kg EpoD for 3 months significantly reduced this MC1-reactive Tau pathology, which is consistent with previous findings (Zhang et al., 2012; Barten et al., 2012).

47

Mechanisms underlying the beneficial effects of EpoD on the amelioration of tau pathology remain unclear. Since somatodendritic mislocalization of tau is accompanied by pathological features of tau such as hyperphosphorylation and aggregation of tau (Zempel and Mandelkow 2014), it is plausible that EpoD could reduce mislocalization of tau into the somatodendritc compartment, lowering risk of developing tau pathology. EpoD is shown to improve MT-based active transport in a tauopathy mouse model (Zhang et al, 2012). It is also possible that the effect of EpoD on improvement of active transport might contribute to amelioration of tau pathology because impaired active transport can lead to exacerbation of hyperphosphorylation and aggregation of tau (Falzone et al., 2010).

Our novel finding that the AIS length is reduced in response to increased neural activity in human iPSC-derived neurons is consistent with the notion that the AIS is a target for homeostatic plasticity mechanisms against changes in neural activity (Grubb and Burrone, 2010; Kuba et al., 2010; Evans et al., 2013). Reduction in the AIS length can be explained by the hypothesis that neurons become less excitable upon prolonged increased neural activity and require stronger stimulation to fire. Interestingly, unlike rodent cultured neurons, human neurons changed the AIS length rather than its location. This discrepancy might stem from different mechanisms underlying cytoskeletal rearrangement for AIS plasticity in human neurons compared to rodent neurons which require L-type calcium channels and calcineurin activation for AIS rearrangement (Evans et al., 2013) since composition of the AIS and its plasticity vary across different neuronal subtypes (Lorincz and Nusser, 2008; Evans et al., 2013).

We found that the AIS of V337M tau neurons started more distally than WT neurons. One possible interpretation would be that hyperexcitability in V337M neurons (unpublished data) leads to AIS shift and shortening as a homeostatic plasticity even in the condition without stimulation. On the other hand, this baseline change of AIS property in V337M tau neurons

might impair its AIS plasticity when external stimulation is applied. This was indeed the case in which the AIS of V337M neurons failed to change its length but showed proximal shift. It is conceivable that this AIS relocation towards the soma might contribute to further increase intrinsic excitability, leading to hyperexcitability in network levels as observed in AD mouse models (Roberson et al., 2007; Roberson et al., 2011; DeVos et al., 2013).

CHAPTER 6

Future Directions

To explore mechanisms of acetylated tau-mediated AIS destabilization.

The current study demonstrated that acetylated tau increased MT dynamics and reduced the levels of AnkG and βIV-spectrin in the AIS. How acetylated tau leads to destabilization of the AIS can further be studied. A portion of K274/281Q tau appears to be detached from MTs and can therefore bind to other cytoskeleton in the AIS that does not normally interact with WT tau. This aberrant binding of K274/281Q tau might inhibit clustering of AIS cytoskeleton. Co-immunoprecipitation of WT and K274/281Q tau can be performed to examine whether their binding affinity for AIS cytoskeleton differs. Whether destabilization of AnkG and βIV-spectrin leads to that of MTs can be determined by knockdown of AnkG or βIV-spectrin by RNAi and then measuring MT dynamics in the AIS in primary neurons. Immunostaining of AnkG or βIV-spectrin after MT-stabilizing drug EpoD injection in tauKQ transgenic mice can determine whether MT stability is critical for maintaining steady levels of AnkG or βIV-spectrin.

To explore neuronal excitability in human V337M tau neurons.

The current study demonstrated that both static and dynamic features of the AIS were altered in human iPSC-derived V337M tau neurons compared to WT neurons. AIS location was shifted distally and activity-dependent shortening of the AIS did not occur in human V337M tau neurons. Neuronal excitability of human V337 tau neurons that can be affected by the altered AIS characteristics needs more investigation. The AIS is the subcellular compartment that initiates action potentials because it has high density of Na^+ channels which makes it the lowest threshold site for initiation of action potentials. Of note, distinct distribution of

subtypes of Na^+ channels within the AIS is the key to determining the properties of action potentials (Hu et al., 2009), suggesting the importance of location of Na^+ channels in neuronal excitability. Studying the role of AIS in neuronal excitability in cultured neurons can be limited due to the variability of ion channel composition at the AIS across different subtypes of neurons (Lorincz and Nusser, 2008). Using human iPSC-derived neurons can bypass this obstacle because they are homogenous glutamatergic excitatory neurons. To compare intrinsic excitability of WT and V337M tau neurons, current threshold for generating action potential and firing frequency as well as basic membrane properties such as membrane resistance and capacitance can be analyzed. Using somatic patch cell recordings, functional details of action potential can be analyzed (Wimmer et al., 2010). The first and second derivatives of action potential trace can help differentiate the somatic and AIS contribution to action potentials. Immunostaining of the AIS with fixation immediately after recording can be analyzed to correlate neuronal excitability and AIS location or length.

To explore ultrastructure of the AIS cytoskeleton in human V337M tau neurons.
Super-resolution imaging studies have revealed detailed spatial relationship between AIS components such as cytoskeleton and ion channels. The platinum replica electron microscopy shows dense submembranous coat of the AIS cytoskeleton, including actin filaments are considered dynamic cytoskeleton that contributes to AIS remodeling upon external stimuli (Jones et al., 2014). The stochastic optical reconstruction microscopy (STORM) uncovers highly organized periodic distribution of actin, βIV-spectrin, and Na^+ channels in the AIS (Xu et al., 2013). To better understand structural abnormality of the AIS in V337M tau neurons, the STORM imaging for AIS cytoskeleton and ion channels can be performed in WT and V337M tau neurons. Collaboration with Ke Xu lab at UC Berkeley has recently been set out to explore ultrastructure of the AIS in WT and V337M tau neurons. Although the

involvement of Ca^{2+} influx and calcineurin in AIS plasticity has been revealed (Grubb and Burrone, 2010; Evans et al., 2013), how these signals lead to cytoskeletal rearrangement in the AIS is still unknown. A recent study by Evans et al. (2015) demonstrates that short-term AIS plasticity displays a shortening of the AIS instead of distal shift of the AIS as described in rat neuronal cultures with prolonged stimulation (Grubb and Burrone 2010; Evans et al., 2013). The longitudinal analysis of STORM imaging of the AIS in stimulated conditions with KCl treatment may provide clues on understanding mechanisms underlying activity-dependent AIS cytoskeletal rearrangement. Dual color STORM imaging of tau and the AIS cytoskeleton can also be performed to explore spatial relationship and possible interactions between tau and cytoskeleton in the AIS.

References

Adams, S. J., Crook, R. J. P., Deture, M., Randle, S. J., Innes, A. E., Yu, X. Z., … McGowan, E. (2009). Overexpression of wild-type murine tau results in progressive tauopathy and neurodegeneration. *The American Journal of Pathology*, *175*(4), 1598–1609. http://doi.org/10.2353/ajpath.2009.090462

Akhmanova, A., & Steinmetz, M. O. (2008). Tracking the ends: a dynamic protein network controls the fate of microtubule tips. *Nature Reviews. Molecular Cell Biology*, *9*(4), 309–22. http://doi.org/10.1038/nrm2369

Applegate, K. T., Besson, S., Matov, A., Bagonis, M. H., Jaqaman, K., & Danuser, G. (2011). plusTipTracker: Quantitative image analysis software for the measurement of microtubule dynamics. *Journal of Structural Biology*, *176*(2), 168–84. http://doi.org/10.1016/j.jsb.2011.07.009

Aronov, S., Aranda, G., Behar, L., & Ginzburg, I. (2001). Axonal tau mRNA localization coincides with tau protein in living neuronal cells and depends on axonal targeting signal. *The Journal of Neuroscience : The Official Journal of the Society for Neuroscience*, *21*(17), 6577–6587. http://doi.org/10.1016/j.neuron.2011.04.009

Arriagada, P. V, Growdon, J. H., Hedley-Whyte, E. T., & Hyman, B. T. (1992). Neurofibrillary tangles but not senile plaques parallel duration and severity of Alzheimer's disease. *Neurology*, *42*(3 Pt 1), 631–639. http://doi.org/10.1212/WNL.42.3.631

Aubry S, Shin W, Crary JF, Lefort R, Qureshi YH, Lefebvre C, Califano A, Shelanski ML (2015) Assembly and interrogation of Alzheimer's disease genetic networks reveal novel regulators of progression. *PLoS One* 10:e0120352.

Ballatore, C., Lee, V. M.-Y., & Trojanowski, J. Q. (2007). Tau-mediated neurodegeneration in Alzheimer's disease and related disorders. *Nature Reviews. Neuroscience*, *8*, 663–672. http://doi.org/10.1038/nrn2194

Bancher, C., Brunner, C., Lassmann, H., Budka, H., Jellinger, K., Wiche, G., … Wisniewski, H. M. (1989). Accumulation of abnormally phosphorylated tau precedes the formation of neurofibrillary tangles in Alzheimer's disease. *Brain Research*, *477*(1-2), 90–99. http://doi.org/10.1016/0006-8993(89)91396-6

Barten, D. M., Fanara, P., Andorfer, C., Hoque, N., Wong, P. Y. A., Husted, K. H., … Albright, C. F. (2012). Hyperdynamic microtubules, cognitive deficits, and pathology are improved in tau transgenic mice with low doses of the microtubule-stabilizing agent BMS-241027. *The Journal of Neuroscience : The Official Journal of the Society for Neuroscience*, *32*(21), 7137–45. http://doi.org/10.1523/JNEUROSCI.0188-12.2012

Baugh, C. M., Stamm, J. M., Riley, D. O., Gavett, B. E., Shenton, M. E., Lin, A., … Stern, R. A. (2012). Chronic traumatic encephalopathy: Neurodegeneration following repetitive concussive and subconcussive brain trauma. *Brain Imaging and Behavior*, *6*(2), 244–254. http://doi.org/10.1007/s11682-012-9164-5

Berg, L., McKeel, D. W., Miller, J. P., Baty, J., & Morris, J. C. (1993). Neuropathological indexes of Alzheimer's disease in demented and nondemented persons aged 80 years and older. *Archives of Neurology*, *50*(4), 349–358. http://doi.org/10.1001/archneur.1993.00540040011008

Biernat, J., Gustke, N., Drewes, G., Mandelkow, E. M., & Mandelkow, E. (1993). Phosphorylation of Ser262 strongly reduces binding of tau to microtubules: distinction between PHF-like immunoreactivity and microtubule binding. *Neuron*, *11*(1), 153–163. http://doi.org/10.1016/0896-6273(93)90279-Z

Binder, L. I., Frankfurter, A., & Rebhun, L. I. (1985). The distribution of tau in the mammalian central nervous system. *Journal of Cell Biology*, *101*, 1371–1378. http://doi.org/10.1083/jcb.101.4.1371

Borchelt, D. R., Davis, J., Fischer, M., Lee, M. K., Slunt, H. H., Ratovitsky, T., … Price, D. L. (1996). A vector for expressing foreign genes in the brains and hearts of transgenic mice. *Genetic Analysis - Biomolecular Engineering*, *13*(6), 159–163. http://doi.org/10.1016/S1050-3862(96)00167-2

Braak, H., Alafuzoff, I., Arzberger, T., Kretzschmar, H., & Tredici, K. (2006). Staging of Alzheimer disease-associated neurofibrillary pathology using paraffin sections and immunocytochemistry. *Acta Neuropathologica*, *112*(4), 389–404. http://doi.org/10.1007/s00401-006-0127-z

Braak, H., & Braak, E. (1991). Neuropathological stageing of Alzheimer-related changes. *Acta Neuropathologica*, *82*(4), 239–259. http://doi.org/10.1007/BF00308809

Brion, J. P. (1992). The pathology of the neuronal cytoskeleton in Alzheimer's disease. In *Biochimica et Biophysica Acta - Protein Structure and Molecular Enzymology* (Vol. 1160, pp. 134–142). http://doi.org/10.1016/0167-4838(92)90047-H

Buffington, S. a, & Rasband, M. N. (2011). The axon initial segment in nervous system disease and injury. *The European Journal of Neuroscience*, *34*, 1609–19. http://doi.org/10.1111/j.1460-9568.2011.07875.x

Bullmann, T., Holzer, M., Mori, H., & Arendt, T. (2009). Pattern of tau isoforms expression during development in vivo. *International Journal of Developmental Neuroscience*, *27*(6), 591–597. http://doi.org/10.1016/j.ijdevneu.2009.06.001

Bunker, J. M., Wilson, L., Jordan, M. A., & Feinstein, S. C. (2004). Modulation of microtubule dynamics by tau in living cells: implications for development and neurodegeneration. *Molecular Biology of the Cell*, *15*(6), 2720–8. http://doi.org/10.1091/mbc.E04-01-0062

Busciglio, J., Lorenzo, A., Yeh, J., & Yankner, B. A. (1995). beta-amyloid fibrils induce tau phosphorylation and loss of microtubule binding. *Neuron*, *14*(4), 879–888. http://doi.org/10.1016/0896-6273(95)90232-5

Cohen, T. J., Guo, J. L., Hurtado, D. E., Kwong, L. K., Mills, I. P., Trojanowski, J. Q., & Lee, V. M. Y. (2011). The acetylation of tau inhibits its function and promotes pathological tau aggregation. *Nature Communications*, *2*, 252. http://doi.org/10.1038/ncomms1255

Conde, C., & Cáceres, A. (2009). Microtubule assembly, organization and dynamics in axons and dendrites. *Nature Reviews. Neuroscience*, *10*(5), 319–332. http://doi.org/10.1038/nrn2631

Cook, C., Carlomagno, Y., Gendron, T. F., Dunmore, J., Scheffel, K., Stetler, C., … Petrucelli, L. (2014). Acetylation of the KXGS motifs in tau is a critical determinant in modulation of tau aggregation and clearance. *Human Molecular Genetics*, *23*(1), 104–116. http://doi.org/10.1093/hmg/ddt402

Coppola, G., Chinnathambi, S., Lee, J. J., Dombroski, B. A., Baker, M. C., Soto-ortolaza, A. I., … Geschwind, D. H. (2012). Evidence for a role of the rare p.A152T variant in mapt in increasing the risk for FTD-spectrum and Alzheimer's diseases. *Human Molecular Genetics*, *21*(15), 3500–3512. http://doi.org/10.1093/hmg/dds161

Dawson, H. N., Ferreira, A., Eyster, M. V, Ghoshal, N., Binder, L. I., & Vitek, M. P. (2001). Inhibition of neuronal maturation in primary hippocampal neurons from tau deficient mice. *Journal of Cell Science*, *114*(Pt 6), 1179–1187.

Delaère, P., Duyckaerts, C., He, Y., Piette, F., & Hauw, J. J. (1991). Subtypes and differential laminar distributions of βA4 deposits in Alzheimer's disease: relationship with the intellectual status of 26 cases. *Acta Neuropathologica*, *81*(3), 328–335. http://doi.org/10.1007/BF00305876

DeVos, S. L., Goncharoff, D. K., Chen, G., Kebodeaux, C. S., Yamada, K., Stewart, F. R., … Miller, T. M. (2013). Antisense reduction of tau in adult mice protects against seizures. *The Journal of Neuroscience : The Official Journal of the Society for Neuroscience*, *33*(31), 12887–97. http://doi.org/10.1523/JNEUROSCI.2107-13.2013

Dickey, C. A., Kamal, A., Lundgren, K., Klosak, N., Bailey, R. M., Dunmore, J., … Petrucelli, L. (2007). The high-affinity HSP90-CHIP complex recognizes and selectively degrades phosphorylated tau client proteins. *Journal of Clinical Investigation*, *117*(3), 648–658. http://doi.org/10.1172/JCI29715

Dickson, D. W., Kouri, N., Murray, M. E., & Josephs, K. A. (2011). Neuropathology of frontotemporal lobar degeneration-Tau (FTLD-Tau). In *Journal of Molecular Neuroscience* (Vol. 45, pp. 384–389). http://doi.org/10.1007/s12031-011-9589-0

Dickson, D. W., Rademakers, R., & Hutton, M. L. (2007). Progressive supranuclear palsy: pathology and genetics. *Brain Pathology (Zurich, Switzerland)*, *17*(1), 74–82. http://doi.org/10.1111/j.1750-3639.2007.00054.x

Dixit, R., Ross, J. L., Goldman, Y. E., & Holzbaur, E. L. F. (2008). Differential regulation of dynein and kinesin motor proteins by tau. *Science (New York, N.Y.)*, *319*(5866), 1086–1089. http://doi.org/10.1126/science.1152993

Evans, M. D., Sammons, R. P., Lebron, S., Dumitrescu, A. S., Watkins, T. B. K., Uebele, V. N., … Grubb, M. S. (2013). Calcineurin signaling mediates activity-dependent relocation of the axon initial segment. *The Journal of Neuroscience : The Official Journal of the Society for Neuroscience*, *33*(16), 6950–63. http://doi.org/10.1523/JNEUROSCI.0277-13.2013

Evans MD, Dumitrescu AS, Kruijssen DLH, Taylor SE, Grubb MS (2015). Rapid modulation of axon initial segment length influences repetitive spike firing. *Cell Reports (in press)*

Falzone, T. L., Gunawardena, S., McCleary, D., Reis, G. F., & Goldstein, L. S. B. (2010). Kinesin-1 transport reductions enhance human tau hyperphosphorylation, aggregation and neurodegeneration in animal models of tauopathies. *Human Molecular Genetics*, *19*(22), 4399–4408. http://doi.org/10.1093/hmg/ddq363

Fanara, P., Husted, K. H., Selle, K., Wong, P. Y. A., Banerjee, J., Brandt, R., & Hellerstein, M. K. (2010). Changes in microtubule turnover accompany synaptic plasticity and memory formation in response to contextual fear conditioning in mice. *Neuroscience*, *168*(1), 167–178. http://doi.org/10.1016/j.neuroscience.2010.03.031

Farias, G. A., Munoz, J. P., Garrido, J., & Maccioni, R. B. (2002). Tubulin, actin, and tau protein interactions and the study of their macromolecular assemblies. *Journal of Cellular Biochemistry*, *85*(2), 315–324. http://doi.org/10.1002/jcb.10133

Frandemiche, M. L., De Seranno, S., Rush, T., Borel, E., Elie, A., Arnal, I., … Buisson, A. (2014). Activity-dependent tau protein translocation to excitatory synapse is disrupted by exposure to amyloid-Beta oligomers. *J Neurosci*, *34*(17), 6084–6097. http://doi.org/10.1523/JNEUROSCI.4261-13.2014

Fulga, T. A., Elson-Schwab, I., Khurana, V., Steinhilb, M. L., Spires, T. L., Hyman, B. T., & Feany, M. B. (2007). Abnormal bundling and accumulation of F-actin mediates tau-induced neuronal degeneration in vivo. *Nature Cell Biology*, *9*(2), 139–148. http://doi.org/10.1038/ncb1528

Goedert, M., Ghetti, B., & Spillantini, M. G. (2012). Frontotemporal dementia: implications for understanding Alzheimer disease. *Cold Spring Harbor Perspectives in Medicine*, *2*(2), a006254. http://doi.org/10.1101/cshperspect.a006254

Gong, C. X., Shaikh, S., Wang, J. Z., Zaidi, T., Grundke-Iqbal, I., & Iqbal, K. (1995). Phosphatase activity toward abnormally phosphorylated tau: decrease in Alzheimer disease brain. *Journal of Neurochemistry*, *65*(2), 732–738. http://doi.org/10.1046/j.1471-4159.1995.65020732.x

Gong, C.-X., Liu, F., Grundke-Iqbal, I., & Iqbal, K. (2005). Post-translational modifications of tau protein in Alzheimer's disease. *Journal of Neural Transmission (Vienna, Austria : 1996)*, *112*(6), 813–838. http://doi.org/10.1007/s00702-004-0221-0

Götz, J., Probst, A., Spillantini, M. G., Schäfer, T., Jakes, R., Bürki, K., & Goedert, M. (1995). Somatodendritic localization and hyperphosphorylation of tau protein in transgenic mice expressing the longest human brain tau isoform. *The EMBO Journal*, *14*(7), 1304–1313.

Grinberg, L. T., Wang, X., Wang, C., Sohn, P. D., Theofilas, P., Sidhu, M., … Seeley, W. W. (2013). Argyrophilic grain disease differs from other tauopathies by lacking tau acetylation. *Acta Neuropathologica*, *125*, 581–593. http://doi.org/10.1007/s00401-013-1080-2

Grubb, M. S., & Burrone, J. (2010). Activity-dependent relocation of the axon initial segment fine-tunes neuronal excitability. *Nature*, *465*(7301), 1070–4. http://doi.org/10.1038/nature09160

Hansson, O., Zetterberg, H., Buchhave, P., Londos, E., Blennow, K., & Minthon, L. (2006). Association between CSF biomarkers and incipient Alzheimer's disease in patients with mild cognitive impairment: a follow-up study. *The Lancet Neurology*. http://doi.org/10.1016/S1474-4422(06)70355-6

Hayashi, K., Suzuki, A., Hirai, S.-I., Kurihara, Y., Hoogenraad, C. C., & Ohno, S. (2011). Maintenance of Dendritic Spine Morphology by Partitioning-Defective 1b through Regulation of Microtubule Growth. *The Journal of Neuroscience : The Official Journal of the Society for Neuroscience*, *31*(34), 12094–12103. http://doi.org/10.1523/JNEUROSCI.0751-11.2011

He, H. J., Wang, X. S., Pan, R., Wang, D. L., Liu, M. N., & He, R. Q. (2009). The proline-rich domain of tau plays a role in interactions with actin. *BMC Cell Biology*, *10*, 81. http://doi.org/10.1186/1471-2121-10-81

Hecht, A., Laroche, T., Strahl-Bolsinger, S., Gasser, S. M., & Grunstein, M. (1995). Histone H3 and H4 N-termini interact with SIR3 and SIR4 proteins: a molecular model for the formation of heterochromatin in yeast. *Cell*, *80*(4), 583–592. http://doi.org/10.1016/0092-8674(95)90512-X

Hedstrom, K. L., Ogawa, Y., & Rasband, M. N. (2008). AnkyrinG is required for maintenance of the axon initial segment and neuronal polarity. *Journal of Cell Biology*, *183*(4), 635–640. http://doi.org/10.1083/jcb.200806112

Hirokawa, N., Funakoshi, T., Sato-Harada, R., & Kanai, Y. (1996). Selective stabilization of tau in axons and microtubule-associated protein 2C in cell bodies and dendrites contributes to polarized localization of cytoskeletal proteins in mature neurons. *Journal of Cell Biology*, *132*(4), 667–679. http://doi.org/10.1083/jcb.132.4.667

Holth, J. K., Bomben, V. C., Reed, J. G., Inoue, T., Younkin, L., Younkin, S. G., … Noebels, J. L. (2013). Tau loss attenuates neuronal network hyperexcitability in mouse and Drosophila genetic models of epilepsy. *Journal of Neuroscience*, *33*(4), 1651–1659. http://doi.org/10.1523/JNEUROSCI.3191-12.2013

Hu, W., Tian, C., Li, T., Yang, M., Hou, H., & Shu, Y. (2009). Distinct contributions of Na(v)1.6 and Na(v)1.2 in action potential initiation and backpropagation. *Nature Neuroscience*, *12*(8), 996–1002. http://doi.org/10.1038/nn.2359

Hutton, M., Lendon, C. L., Rizzu, P., Baker, M., Froelich, S., Houlden, H., … Heutink, P. (1998). Association of missense and 5'-splice-site mutations in tau with the inherited dementia FTDP-17. *Nature*, *393*(6686), 702–705. http://doi.org/10.1038/31508

Iqbal, K., Del C. Alonso, A., Chen, S., Chohan, M. O., El-Akkad, E., Gong, C. X., … Grundke-Iqbal, I. (2005). Tau pathology in Alzheimer disease and other tauopathies. *Biochimica et Biophysica Acta - Molecular Basis of Disease*. http://doi.org/10.1016/j.bbadis.2004.09.008

Irwin, D. J., Cohen, T. J., Grossman, M., Arnold, S. E., Xie, S. X., Lee, V. M. Y., & Trojanowski, J. Q. (2012). Acetylated tau, a novel pathological signature in Alzheimer's disease and other tauopathies. *Brain*, *135*, 807–818. http://doi.org/10.1093/brain/aws013

Ishiguro, K., Kobayashi, S., Omori, A., Takamatsu, M., Yonekura, S., Anzai, K., … Uchida, T. (1994). Identification of the 23 kDa subunit of tau protein kinase II as a putative activator of cdk5 in bovine brain. *FEBS Letters*, *342*(2), 203–208. http://doi.org/10.1016/0014-5793(94)80501-6

Ishiguro, K., Shiratsuchi, A., Sato, S., Omori, A., Arioka, M., Kobayashi, S., … Imahori, K. (1993). Glycogen synthase kinase 3 beta is identical to tau protein kinase I generating several epitopes of paired helical filaments. *FEBS Letters*, *325*(3), 167–172.

Ittner, L. M., & Götz, J. (2011). Amyloid-β and tau--a toxic pas de deux in Alzheimer's disease. *Nature Reviews. Neuroscience*, *12*, 65–72. http://doi.org/10.1038/nrn2967

Ittner, L. M., Ke, Y. D., Delerue, F., Bi, M., Gladbach, A., van Eersel, J., … Götz, J. (2010a). Dendritic function of tau mediates amyloid-beta toxicity in Alzheimer's disease mouse models. *Cell*, *142*, 387–397. http://doi.org/10.1016/j.cell.2010.06.036

Ittner, L. M., Ke, Y. D., Delerue, F., Bi, M., Gladbach, A., van Eersel, J., … Götz, J. (2010b). Dendritic function of tau mediates amyloid-beta toxicity in Alzheimer's disease mouse models. *Cell*, *142*(3), 387–397. http://doi.org/10.1016/j.cell.2010.06.036

Janke, C., & Kneussel, M. (2010). Tubulin post-translational modifications: Encoding functions on the neuronal microtubule cytoskeleton. *Trends in Neurosciences*. http://doi.org/10.1016/j.tins.2010.05.001

Jenkins, S. M., & Bennett, V. (2001). Ankyrin-G coordinates assembly of the spectrin-based membrane skeleton, voltage-gated sodium channels, and L1 CAMs at Purkinje neuron initial segments. *Journal of Cell Biology*, *155*(5), 739–745. http://doi.org/10.1083/jcb.200109026

Jicha, G. A., Bowser, R., Kazam, I. G., & Davies, P. (1997). Alz-50 and MC-1, a new monoclonal antibody raised to paired helical filaments, recognize conformational epitopes on recombinant tau. *Journal of Neuroscience Research*, *48*(2), 128–32.

Jicha, G. A., Weaver, C., Lane, E., Vianna, C., Kress, Y., Rockwood, J., & Davies, P. (1999). cAMP-dependent protein kinase phosphorylations on tau in Alzheimer's disease. *The Journal of Neuroscience : The Official Journal of the Society for Neuroscience*, *19*(17), 7486–7494.

Jones, S. L., Korobova, F., & Svitkina, T. (2014). Axon initial segment cytoskeleton comprises a multiprotein submembranous coat containing sparse actin filaments. *Journal of Cell Biology*, *205*, 67–81. http://doi.org/10.1083/jcb.201401045

Kanai, Y., & Hirokawa, N. (1995). Sorting mechanisms of tau and MAP2 in neurons: suppressed axonal transit of MAP2 and locally regulated microtubule binding. *Neuron*, *14*(2), 421–432. http://doi.org/10.1016/0896-6273(95)90298-8

Kar, S., Fan, J., Smith, M. J., Goedert, M., & Amos, L. A. (2003). Repeat motifs of tau bind to the insides of microtubules in the absence of taxol. *EMBO Journal*, *22*(1), 70–77. http://doi.org/10.1093/emboj/cdg001

Kim, G. W., & Yang, X. J. (2011). Comprehensive lysine acetylomes emerging from bacteria to humans. *Trends in Biochemical Sciences*. http://doi.org/10.1016/j.tibs.2010.10.001

King, M. E., Kan, H. M., Baas, P. W., Erisir, A., Glabe, C. G., & Bloom, G. S. (2006). Tau-dependent microtubule disassembly initiated by prefibrillar ??-amyloid. *Journal of Cell Biology*, *175*(4), 541–546. http://doi.org/10.1083/jcb.200605187

Kishi, M., Pan, Y. A., Crump, J. G., & Sanes, J. R. (2005). Mammalian SAD kinases are required for neuronal polarization. *Science (New York, N.Y.)*, *307*(5711), 929–932. http://doi.org/10.1126/science.1107403

Komada, M., & Soriano, P. (2002). ??IV-spectrin regulates sodium channel clustering through ankyrin-G at axon initial segments and nodes of Ranvier. *Journal of Cell Biology*, *156*(2), 337–348. http://doi.org/10.1083/jcb.200110003

Konishi, Y., & Setou, M. (2009). Tubulin tyrosination navigates the kinesin-1 motor domain to axons. *Nature Neuroscience*, *12*(5), 559–567. http://doi.org/10.1038/nn.2314

Kuba, H., Oichi, Y., & Ohmori, H. (2010). Presynaptic activity regulates Na(+) channel distribution at the axon initial segment. *Nature*, *465*(7301), 1075–8. http://doi.org/10.1038/nature09087

Lacroix, B., Van Dijk, J., Gold, N. D., Guizetti, J., Aldrian-Herrada, G., Rogowski, K., … Janke, C. (2010). Tubulin polyglutamylation stimulates spastin-mediated microtubule severing. *Journal of Cell Biology*, *189*(6), 945–954. http://doi.org/10.1083/jcb.201001024

Lee, M. K., & Cleveland, D. W. (1994). Neurofilament function and dysfunction: involvement in axonal growth and neuronal disease. *Current Opinion in Cell Biology*, *6*(1), 34–40. http://doi.org/10.1016/0955-0674(94)90113-9

Lee, V. M., Goedert, M., & Trojanowski, J. Q. (2001). Neurodegenerative tauopathies. *Annual Review of Neuroscience*, *24*, 1121–1159. http://doi.org/10.1016/S0896-6273(00)81106-X

Leterrier, C., Vacher, H., Fache, M.-P., d'Ortoli, S. A., Castets, F., Autillo-Touati, A., & Dargent, B. (2011). End-binding proteins EB3 and EB1 link microtubules to ankyrin G in the axon initial segment. *Proceedings of the National Academy of Sciences of the United States of America*, *108*(21), 8826–31. http://doi.org/10.1073/pnas.1018671108

Lewis, J., Dickson, D. W., Lin, W. L., Chisholm, L., Corral, A., Jones, G., … McGowan, E. (2001). Enhanced neurofibrillary degeneration in transgenic mice expressing mutant tau and APP. *Science (New York, N.Y.)*, *293*(5534), 1487–1491. http://doi.org/10.1126/science.1058189

Li, X., Kumar, Y., Zempel, H., Mandelkow, E.-M., Biernat, J., & Mandelkow, E. (2011). Novel diffusion barrier for axonal retention of Tau in neurons and its failure in neurodegeneration. *The EMBO Journal*. http://doi.org/10.1038/emboj.2011.376

Liu, F., Grundke-Iqbal, I., Iqbal, K., & Gong, C. X. (2005). Contributions of protein phosphatases PP1, PP2A, PP2B and PP5 to the regulation of tau phosphorylation. *European Journal of Neuroscience*, *22*(8), 1942–1950. http://doi.org/10.1111/j.1460-9568.2005.04391.x

Lorincz, A., & Nusser, Z. (2008). Cell-type-dependent molecular composition of the axon initial segment. *The Journal of Neuroscience : The Official Journal of the Society for Neuroscience*, *28*(53), 14329–14340. http://doi.org/10.1523/JNEUROSCI.4833-08.2008

Lu, M., & Kosik, K. S. (2001). Competition for microtubule-binding with dual expression of tau missense and splice isoforms. *Molecular Biology of the Cell*, *12*(1), 171–84.

Luo, J., Li, M., Tang, Y., Laszkowska, M., Roeder, R. G., & Gu, W. (2004). Acetylation of p53 augments its site-specific DNA binding both in vitro and in vivo. *Proceedings of the National Academy of Sciences of the United States of America*, *101*(8), 2259–2264. http://doi.org/10.1073/pnas.0308762101

Mandell, J. W., & Banker, G. A. (1995). The microtubule cytoskeleton and the development of neuronal polarity. *Neurobiology of Aging*, *16*(3), 229–37; discussion 238.

Maniar, T. A., Kaplan, M., Wang, G. J., Shen, K., Wei, L., Shaw, J. E., … Bargmann, C. I. (2011). UNC-33 (CRMP) and ankyrin organize microtubules and localize kinesin to polarize axon-dendrite sorting. *Nature Neuroscience*. http://doi.org/10.1038/nn.2970

Martin, L., Latypova, X., Wilson, C. M., Magnaudeix, A., Perrin, M. L., & Terro, F. (2013). Tau protein phosphatases in Alzheimer's disease: The leading role of PP2A. *Ageing Research Reviews*. http://doi.org/10.1016/j.arr.2012.06.008

Mattsson, N., Blennow, K., & Zetterberg, H. (2009). CSF biomarkers: Pinpointing alzheimer pathogenesis. In *Annals of the New York Academy of Sciences* (Vol. 1180, pp. 28–35). http://doi.org/10.1111/j.1749-6632.2009.04944.x

Min, S. W., Cho, S. H., Zhou, Y., Schroeder, S., Haroutunian, V., Seeley, W. W., … Gan, L. (2010). Acetylation of tau inhibits its degradation and contributes to tauopathy. *Neuron*, *67*, 953–966. http://doi.org/10.1016/j.neuron.2010.08.044

Min SW, Chen X, Tracy T, Li Y, Zhou Y, Wang C, Shirakawa K, Minami S, Defensor E, Mok SA , Sohn PD, Schilling B, Cong X, Ellerby L, Gibson B, Johnson J, Krogan N, Shamloo M, Gestwicki J, Masliah E, Verdin E, Gan L (2015). Critical Role of Acetylation in Tau-Mediated Neurodegeneration and Cognitive Deficits. *Nature Medicine* (*in press*)

Morita, T., & Sobuě, K. (2009). Specification of neuronal polarity regulated by local translation of CRMP2 and tau via the mTOR-p70S6K pathway. *Journal of Biological Chemistry*, *284*(40), 27734–27745. http://doi.org/10.1074/jbc.M109.008177

Morris, M., Maeda, S., Vossel, K., & Mucke, L. (2011). The Many Faces of Tau. *Neuron*. http://doi.org/10.1016/j.neuron.2011.04.009

Morris M, Knudsen GM, Maeda S, Trinidad JC, Ioanoviciu A, Burlingame AL, Mucke L. (2015) Tau post-translational modifications in wild-type and human amyloid precursor protein transgenic mice. *Nature Neuroscience*, 18(8):1183-9. doi: 10.1038/nn.4067.

Nakata, T., Niwa, S., Okada, Y., Perez, F., & Hirokawa, N. (2011). Preferential binding of a kinesin-1 motor to GTP-tubulin-rich microtubules underlies polarized vesicle transport. *The Journal of Cell Biology*, *194*(2), 245–55. http://doi.org/10.1083/jcb.201104034

Noble, W., Olm, V., Takata, K., Casey, E., Mary, O., Meyerson, J., … Duff, K. (2003). Cdk5 is a key factor in tau aggregation and tangle formation in vivo. *Neuron*, *38*(4), 555–565. http://doi.org/10.1016/S0896-6273(03)00259-9

Palay, S. L., Sotelo, C., Peters, A., & Orkand, P. M. (1968). The axon hillock and the initial segment. *Journal of Cell Biology*, *38*, 193–201. http://doi.org/10.1083/jcb.38.1.193

Panda, D., Samuel, J. C., Massie, M., Feinstein, S. C., & Wilson, L. (2003). Differential regulation of microtubule dynamics by three- and four-repeat tau: implications for the onset of neurodegenerative disease. *Proceedings of the National Academy of Sciences of the United States of America*, *100*(16), 9548–53. http://doi.org/10.1073/pnas.1633508100

Perkins, D. N., Pappin, D. J., Creasy, D. M., & Cottrell, J. S. (1999). Probability-based protein identification by searching sequence databases using mass spectrometry data. *Electrophoresis*, *20*(18), 3551–3567. http://doi.org/10.1002/(SICI)1522-2683(19991201)20:18<3551::AID-ELPS3551>3.0.CO;2-2

Rasband, M. N. (2010). The axon initial segment and the maintenance of neuronal polarity. *Nature Reviews. Neuroscience*, *11*(8), 552–62. http://doi.org/10.1038/nrn2852

Ren, Q. G., Liao, X. M., Chen, X. Q., Liu, G. P., & Wang, J. Z. (2007). Effects of tau phosphorylation on proteasome activity. *FEBS Letters*, *581*(7), 1521–1528. http://doi.org/10.1016/j.febslet.2007.02.065

Roberson, E. D., Halabisky, B., Yoo, J. W., Yao, J., Chin, J., Yan, F., … Mucke, L. (2011). Amyloid-β/Fyn-induced synaptic, network, and cognitive impairments depend on tau levels in multiple mouse models of Alzheimer's disease. *The Journal of Neuroscience : The Official Journal of the Society for Neuroscience*, *31*(2), 700–711. http://doi.org/10.1523/JNEUROSCI.4152-10.2011

Roberson, E. D., Scearce-Levie, K., Palop, J. J., Yan, F., Cheng, I. H., Wu, T., … Mucke, L. (2007). Reducing endogenous tau ameliorates amyloid beta-induced deficits in an Alzheimer's disease mouse model. *Science (New York, N.Y.)*, *316*(5825), 750–754. http://doi.org/10.1126/science.1141736

Rosenmann, H., Grigoriadis, N., Eldar-Levy, H., Avital, A., Rozenstein, L., Touloumi, O., … Abramsky, O. (2008). A novel transgenic mouse expressing double mutant tau driven by its natural promoter exhibits tauopathy characteristics. *Experimental Neurology*, *212*, 71–84. http://doi.org/10.1016/j.expneurol.2008.03.007

Samsonov, A., Yu, J.-Z., Rasenick, M., & Popov, S. V. (2004). Tau interaction with microtubules in vivo. *Journal of Cell Science*, *117*(Pt 25), 6129–6141. http://doi.org/10.1242/jcs.01531

Sayas, C. L., Tortosa, E., Bollati, F., Ram ŕez-R ós, S., Arnal, I., & Avila, J. (2015). Tau regulates the localization and function of End-binding proteins 1 and 3 (EB1/3) in developing neuronal cells. *Journal of Neurochemistry*, *3*, n/a–n/a. http://doi.org/10.1111/jnc.13091

Schilling, B., Rardin, M. J., MacLean, B. X., Zawadzka, A. M., Frewen, B. E., Cusack, M. P., … Gibson, B. W. (2012). Platform-independent and Label-free Quantitation of Proteomic Data Using MS1 Extracted Ion Chromatograms in Skyline: APPLICATION TO PROTEIN ACETYLATION AND PHOSPHORYLATION. *Molecular & Cellular Proteomics*. http://doi.org/10.1074/mcp.M112.017707

Schneider, A., Biernat, J., Von Bergen, M., Mandelkow, E., & Mandelkow, E. M. (1999). Phosphorylation that detaches tau protein from microtubules (Ser262, Ser214) also protects it against aggregation into Alzheimer paired helical filaments. *Biochemistry*, *38*(12), 3549–3558. http://doi.org/10.1021/bi981874p

Shilov, I. V, Seymour, S. L., Patel, A. A., Loboda, A., Tang, W. H., Keating, S. P., … Schaeffer, D. A. (2007). The Paragon Algorithm, a next generation search engine that uses sequence temperature values and feature probabilities to identify peptides from tandem mass spectra. *Molecular & Cellular Proteomics : MCP*, *6*(9), 1638–1655. http://doi.org/10.1074/mcp.T600050-MCP200

Song, A. hong, Wang, D., Chen, G., Li, Y., Luo, J., Duan, S., & Poo, M. ming. (2009). A Selective Filter for Cytoplasmic Transport at the Axon Initial Segment. *Cell*, *136*, 1148–1160. http://doi.org/10.1016/j.cell.2009.01.016

Stoothoff, W. H., & Johnson, G. V. W. (2005). Tau phosphorylation: Physiological and pathological consequences. *Biochimica et Biophysica Acta - Molecular Basis of Disease*. http://doi.org/10.1016/j.bbadis.2004.06.017

Sun, X., Wu, Y., Gu, M., Liu, Z., Ma, Y., Li, J., & Zhang, Y. (2014). Selective filtering defect at the axon initial segment in Alzheimer's disease mouse models. *Proceedings of the National Academy of Sciences of the United States of America*, *111*(39), 14271–14276. http://doi.org/10.1073/pnas.1411837111

Tai, H. C., Serrano-Pozo, A., Hashimoto, T., Frosch, M. P., Spires-Jones, T. L., & Hyman, B. T. (2012). The synaptic accumulation of hyperphosphorylated tau oligomers in alzheimer disease is associated with dysfunction of the ubiquitin-proteasome system. *American Journal of Pathology*, *181*(4), 1426–1435. http://doi.org/10.1016/j.ajpath.2012.06.033

Terwel, D., Lasrado, R., Snauwaert, J., Vandeweert, E., Van Haesendonck, C., Borghgraef, P., & Van Leuven, F. (2005). Changed conformation of mutant tau-P301L underlies the moribund tauopathy, absent in progressive, nonlethal axonopathy of tau-4R/2N transgenic mice. *Journal of Biological Chemistry*, *280*(5), 3963–3973. http://doi.org/10.1074/jbc.M409876200

Thies, E., & Mandelkow, E.-M. (2007). Missorting of tau in neurons causes degeneration of synapses that can be rescued by the kinase MARK2/Par-1. *The Journal of Neuroscience : The Official Journal of the Society for Neuroscience*, *27*(11), 2896–2907. http://doi.org/10.1523/JNEUROSCI.4674-06.2007

Tsushima H, Emanuele M, Polenghi A, Esposito A, Vassalli M, Barberis A, Difato F, Chieregatti E. (2015) HDAC6 and RhoA are novel players in Abeta-driven disruption of neuronal polarity. *Nature Communications*, 6:7781. doi: 10.1038/ncomms8781.

Vossel, K. A., Zhang, K., Brodbeck, J., Daub, A. C., Sharma, P., Finkbeiner, S., … Mucke, L. (2010). Tau reduction prevents Abeta-induced defects in axonal transport. *Science (New York, N.Y.)*, *330*(6001), 198. http://doi.org/10.1126/science.1194653

Wagner, U., Utton, M., Gallo, J. M., & Miller, C. C. (1996). Cellular phosphorylation of tau by GSK-3 beta influences tau binding to microtubules and microtubule organisation. *Journal of Cell Science*, *109 (Pt 6*, 1537–1543.

Wang, J. Z., Grundke-Iqbal, I., & Iqbal, K. (2007). Kinases and phosphatases and tau sites involved in Alzheimer neurofibrillary degeneration. *European Journal of Neuroscience*, *25*(1), 59–68. http://doi.org/10.1111/j.1460-9568.2006.05226.x

Weingarten, M. D., Lockwood, A. H., Hwo, S. Y., & Kirschner, M. W. (1975). A protein factor essential for microtubule assembly. *Proceedings of the National Academy of Sciences of the United States of America*, *72*(5), 1858–62. http://doi.org/10.1073/pnas.72.5.1858

Wimmer, V. C., Reid, C. A., So, E. Y.-W., Berkovic, S. F., & Petrou, S. (2010). Axon initial segment dysfunction in epilepsy. *The Journal of Physiology*, *588*(Pt 11), 1829–1840. http://doi.org/10.1113/jphysiol.2010.188417

Winckler, B., Forscher, P., & Mellman, I. (1999). A diffusion barrier maintains distribution of membrane proteins in polarized neurons. *Nature*, *397*(6721), 698–701. http://doi.org/10.1038/17806

Xu, K., Zhong, G., & Zhuang, X. (2013). Actin, spectrin, and associated proteins form a periodic cytoskeletal structure in axons. *Science (New York, N.Y.)*, *339*(6118), 452–6. http://doi.org/10.1126/science.1232251

Yoshiyama, Y., Higuchi, M., Zhang, B., Huang, S. M., Iwata, N., Saido, T. C., … Lee, V. M. Y. (2007). Synapse Loss and Microglial Activation Precede Tangles in a P301S Tauopathy Mouse Model. *Neuron*, *53*(3), 337–351. http://doi.org/10.1016/j.neuron.2007.01.010

Yuan, A., Kumar, A., Peterhoff, C., Duff, K., & Nixon, R. A. (2008). Axonal transport rates in vivo are unaffected by tau deletion or overexpression in mice. *The Journal of Neuroscience : The Official Journal of the Society for Neuroscience*, *28*(7), 1682–1687. http://doi.org/10.1523/JNEUROSCI.5242-07.2008

Zempel, H., Luedtke, J., Kumar, Y., Biernat, J., Dawson, H., Mandelkow, E., & Mandelkow, E.-M. (2013). Amyloid-β oligomers induce synaptic damage via Tau-dependent microtubule severing by TTLL6 and spastin. *The EMBO Journal*, *32*(22), 2920–37.

Zempel, H., & Mandelkow, E. (2014). Lost after translation: missorting of Tau protein and consequences for Alzheimer disease. *Trends in Neurosciences*, 1–12. http://doi.org/10.1016/j.tins.2014.08.004

Zempel, H., Thies, E., Mandelkow, E., & Mandelkow, E.-M. (2010). Abeta oligomers cause localized Ca(2+) elevation, missorting of endogenous Tau into dendrites, Tau phosphorylation, and destruction of microtubules and spines. *The Journal of Neuroscience : The Official Journal of the Society for Neuroscience*, *30*, 11938–11950. http://doi.org/10.1523/JNEUROSCI.2357-10.2010

Zhang, B., Carroll, J., Trojanowski, J. Q., Yao, Y., Iba, M., Potuzak, J. S., … Brunden, K. R. (2012). The microtubule-stabilizing agent, epothilone D, reduces axonal dysfunction, neurotoxicity, cognitive deficits, and Alzheimer-like pathology in an interventional study with aged tau transgenic mice. *The Journal of Neuroscience : The Official Journal of the Society for Neuroscience*, *32*(11), 3601–11. http://doi.org/10.1523/JNEUROSCI.4922-11.2012

Zhang, B., Maiti, A., Shively, S., Lakhani, F., McDonald-Jones, G., Bruce, J., … Trojanowski, J. Q. (2005). Microtubule-binding drugs offset tau sequestration by stabilizing microtubules and reversing fast axonal transport deficits in a tauopathy model. *Proceedings of the National Academy of Sciences of the United States of America*, *102*(1), 227–231. http://doi.org/10.1073/pnas.0406361102

Zhang, Y., Pak, C., Han, Y., Ahlenius, H., Zhang, Z., Chanda, S., … Südhof, T. C. (2013). Rapid single-step induction of functional neurons from human pluripotent stem cells. *Neuron*, *78*(5), 785–798. http://doi.org/10.1016/j.neuron.2013.05.029

Publishing Agreement

It is the policy of the University to encourage the distribution of all theses, dissertations, and manuscripts. Copies of all UCSF theses, dissertations, and manuscripts will be routed to the library via the Graduate Division. The library will make all theses, dissertations, and manuscripts accessible to the public and will preserve these to the best of their abilities, in perpetuity.

Please sign the following statement:

I hereby grant permission to the Graduate Division of the University of California, San Francisco to release copies of my thesis, dissertation, or manuscript to the Campus Library to provide access and preservation, in whole or in part, in perpetuity.

_____

Author Signature

09 / 30 / 2015

Date